Negative capacitance effects in ferroelectric

Cite as: J. Appl. Phys. 129, 080901 (2021); doi: 10.1063/5.0038971 Submitted: 28 November 2020 · Accepted: 4 February 2021 · Published Online: 25 February 2021







Atanu K. Saha^{a) 📵} and Sumeet K. Gupta 🗓



AFFILIATIONS

School of Electrical and Computer Engineering, Purdue University, West Lafayette, Indiana 47906, USA

^alAuthor to whom correspondence should be addressed: saha26@purdue.edu

ABSTRACT

In a heterogeneous system, ferroelectric materials can exhibit negative capacitance (NC) behavior given that the overall capacitance of the system remains positive. Such NC effects may lead to differential amplification in local potential and can provide an enhanced charge and capacitance response for the whole system compared to their constituents. Such intriguing implications of NC phenomena have prompted the design and exploration of many ferroelectric-based electronic devices to not only achieve an improved performance but potentially also overcome some fundamental limits of standard transistors. However, the microscopic physical origin as well as the true nature of the NC effect, and direct experimental evidence remain elusive and debatable. To that end, in this article, we provide a comprehensive theoretical perspective on the current understanding of the underlying physical mechanism of the NC effect in the ferroelectric material. Based upon the fundamental physics of ferroelectric material, we discuss different assumptions, conditions, and distinct features of the quasi-static NC effect in the single-domain and multi-domain scenarios. While the quasi-static and hysteresis-free NC effect was initially propounded in the context of a single-domain scenario, we highlight that similar effects can be observed in multi-domain FEs with soft domain-wall (DW) displacement. Furthermore, to obtain the soft-DW, the gradient energy coefficient of the FE material is required to be higher as well as the ferroelectric thickness is required to be lower than some critical values. If those requirements are not met, then the DW becomes hard and their displacement would lead to hysteretic NC effects, which are adiabatically irreversible. In addition to the quasi-static NC, we discuss different mechanisms that can potentially lead to the transient NC effects. Furthermore, we discuss different existing experimental results by correlating their distinct features with different types of NC attributes and provide guidelines for new experiments that can potentially provide new insights on unveiling the real origin of NC phenomena.

Published under license by AIP Publishing. https://doi.org/10.1063/5.0038971

I. INTRODUCTION

The notion of negative capacitance (NC) in ferroelectric (FE) based devices has been intriguing many physicists, scientists, and engineers for several decades; 1-26 not only because of the rich underlying physical mechanisms and theoretical explanations associated with such unconventional effects but also due to its potentially groundbreaking implications in the design of low power, steep switching, and aggressively voltage-scalable transistors. 6,17 The nature of the negative capacitance effects in ferroelectrics has been a subject of intense debate. 13-17 In particular, different schools of thought have formed in response to the question of whether or not the capacitance in ferroelectrics can be intrinsically negative. 13-17 On one hand, there have been strong proponents of the idea that ferroelectrics can access their intrinsic negative capacitance paths under certain conditions. On the other hand, there have been several

explanations that indicate that the negative capacitance observed in experiments is either an effective parameter or the result of transient phenomena. 13-17 Irrespective of which notion turns out to be true, there is a convergence amongst the researchers that this effect needs systematic investigation to explore its possible applications in the design of future electronic systems.

In order to introduce the concept of NC in more detail and to provide a proper perspective into the nature of NC effects, let us start from the fundamentals. For a capacitor based on linear dielectrics (i.e., metal-insulator-metal or MIM configuration), its capacitance (C) is a measure of how much static charge (Q) it can store when a voltage (V) is applied between the metal electrodes and is defined as C = Q/V. From there, the stored electrical energy in a capacitor can be obtained as $U = Q^2/(2C)$. To be electrostatically and thermodynamically stable, the capacitance of a system is required to be positive. To understand this, let us hypothetically consider a system exhibiting negative capacitance. In this case, the energy of the system can be represented as the $U = -Q^2/(2|C|)$. This implies that an increase in Q would lead to a decrease in its energy. If such a capacitor is short-circuited, then it would keep building charges spontaneously in the metal plates to minimize its energy. This implies that the system can change its internal energy without any external work, which is a violation of the first law of thermodynamics. Therefore, the electrostatic capacitance of a system must be a positive quantity to ensure thermodynamic stability.

In a more general scenario, when the capacitor is non-linear, the definition of the differential capacitance (C) is more appropriate, which relates the differential change in Q(dQ) with respect to the differential change in V(dV) as C = dQ/dV. While having a stable negative capacitance (dQ/dV < 0) of the system is not physical, an unstable negative capacitance region is indeed theoretically possible if that region is bounded by a positive capacitance (dQ/dV > 0) region. Hence, it is no surprise that the appearance of spontaneous charge (or polarization) in the ferroelectric material contains the signature of an unstable negative capacitance region, while the finiteness of the spontaneous charges signifies a positive capacitance region. Based on a similar rationale, the possibility of capacitance being negative for ferroelectric (FE) materials was first anticipated by Landauer in 1976.

While the requirement that the capacitance must be positive for any system as a whole is universal, the capacitance of a part of the system being negative does not immediately violate any physical laws. In 2000, Bratkovsky and Levanuuk theoretically predicted that the effective capacitance of a multi-domain FE can be negative in the presence of the interfacial dead layer. In this pioneering work, they show that, while the total capacitance of the system (FE layer + dead layer) remains positive, the domain-wall displacement leads to an effective negative capacitance in the FE layer. Later on, in 2006, the same authors experimentally demonstrated this effect for a BTO/SRO/STO system by subtracting the estimated potential drop across the dead layer and revealing the "real" hysteresis loop in the FE layer signifying the presence of effective negative capacitance (NC).

In 2008, Salahuddin and Datta proposed an intriguing concept for overcoming the fundamental limit in the subthreshold swing of a conventional transistor. They suggested that the presence of a negative capacitor in the gate stack of a transistor can provide an amplified internal potential, which can potentially lead to a lower than 60 mV/decade sub-threshold swing in the transistor characteristics at room temperature. In addition, the authors envisioned the utilization of the FE layer as the possible source of NC and proposed the "capacitance matching" theory for obtaining a hysteresis-free operation with maximum amplification of the internal potential."

While the NC effect in FE and its potential application in designing steep switching transistors (NCFETs) looked intriguing, the thrust in this area took a major surge with the discovery of ferroelectricity in HfO₂-based materials, ^{29–32} which are highly CMOS compatible (compared to the conventional perovskite FE). This not only led to the possibilities of practical realization of steep-slope transistors ^{33–39} but has also ushered in the proposal for other FE based devices that utilize the intricate polarization switching

dynamics 40 of the FE materials for memory 41-42 and non-Boolean applications. 43-46 Interestingly, the underlying physics of the NC effect is strongly correlated with the fundamental mechanism of polarization switching in the ferroelectrics. Hence, the NC phenomenon has sparked an immense interest leading to a large body of work aimed to understand the NC effects in FE based devices and its dependence on the material and device parameters.

In this paper, we provide an overview of the current theoretical understanding of the possible origins of NC effects in ferroelectrics and present a perspective on the strengths and limitations of various explanations. We also discuss the relevant experimental works and provide an outlook for what is needed to further understand these intriguing phenomena. The organization of the paper is the following. In Sec. II, we discuss the Landau-Ginzburg-Devonshire formalism of FE materials. In Sec. III, we discuss the quasi-static negative capacitance effect in FE for the single-domain and multi-domain scenario by considering the implications of elastic interaction and FE thickness scaling. In Sec. IV, we discuss another interesting phenomenon that leads to an enhanced (but positive) effective permittivity in FE materials. In Sec. V, we discuss the transient NC effect. Then, we analyze some of the relevant experimental results and their correlation with the different mechanisms of NC effects as well as new experimental methodologies in Sec. VI. In Sec. VII, we provide a brief perspective on different FE materials and examine their possibilities for harnessing hysteresisfree NC effects. Finally, in Sec. VIII, we qualitatively discuss the implication of different NC mechanism and their influence in FEFET characteristics. We summarize our discussion in Sec. IX.

II. FERROELECTRIC CAPACITORS

Microscopically, the ferroelectricity originates from the noncentrosymmetric crystal structure where the spontaneous displacement of atoms (and the corresponding electron gas and ion core) leads to a non-zero spontaneous polarization (P). Therefore, the total spontaneous P in a FE material should be considered as the combination of ionic and electronic polarization. In the simplest scenario, where the spontaneous displacement of atoms is uniaxial (uniaxial FE), the consideration of crystal symmetry provides two possible spontaneous P states depending on the direction of atomic displacement [Figs. 1(a) and 1(b)]. Let us assume that the direction of spontaneous displacement is the \pm z axis ($P_z = P$) and the corresponding P states are -P and +P [Figs. 1(a) and 1(b)]. These -Pand + P states correspond to the minimum of the free energy of a FE unit cell [Fig. 1(c)]. Now, the bi-stability in spontaneous P and the corresponding two minima in its free energy leads to the formation of a double-well-shaped free energy landscape [Fig. 1(c)], which can be represented as Landau's free energy equation [Eq. (1)] as shown below:

$$f_{free} = \frac{1}{2}\alpha P^2 + \frac{1}{4}\beta P^4 + \frac{1}{6}\gamma P^6.$$
 (1)

Here, α , β , and γ are Landau coefficients, where α is negative and γ must be positive. Such a double-well energy landscape suggests that any reduction in P magnitude from its spontaneous value should lead to an increase in free energy, where P=0 corresponds

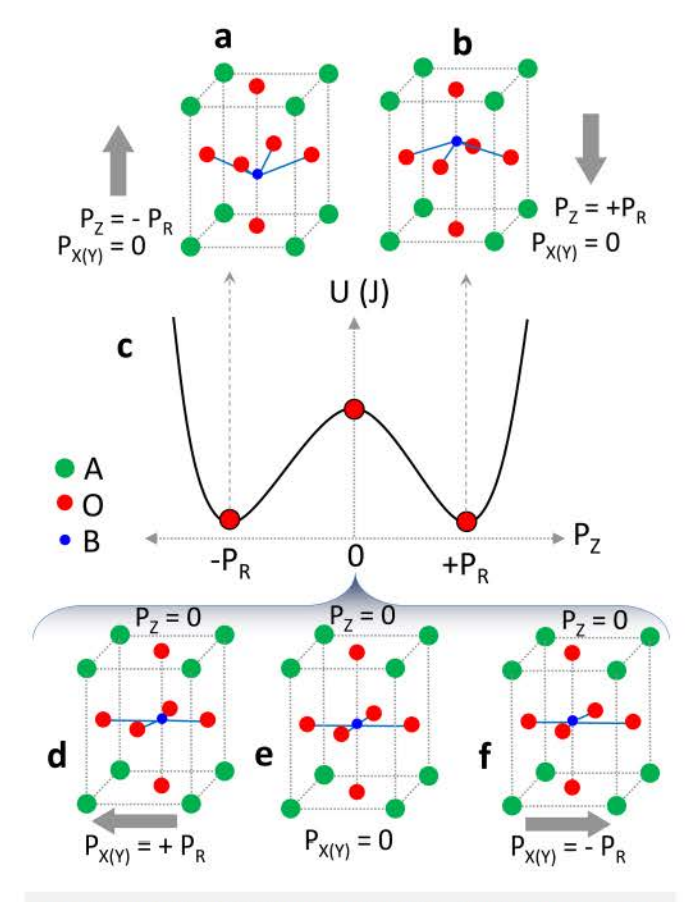


FIG. 1. Ferroelectric ABO₃ tetragonal unit cells (i.e., PbTiO₃) showing spontaneous atomic displacement that correspond to (a) up polarization $(P = P_Z = -P_R)$ and down polarization $(P = P_Z = +P_R)$. Free energy $(U = \int free.dV)$ landscape with respect to polarization (P). (d)–(f) Different atomic configurations in a tetragonal unit cell that corresponds to $P_Z = 0$.

to the energy maxima [Fig. 1(c)]. Here, the P=0 state corresponds to a zero atomic displacement along the z axis, however, may or may not have a finite displacement along the in-plane directions [Figs. 1(d)-1(f)]. It is important to note that, even though the Landau free energy polynomial was originally proposed for a macroscopic polarization, such representation holds true even for a microscopic scenario (i.e., single FE unit cell) as shown in several first-principle studies. 47,48

In addition to the free energy, the presence of an out-of-plane electric field (E) in the FE layer also leads to an energy component called electrostatic energy. The electrostatic energy density (f_{elec}) can be written as $f_{elec} = -E.P.$ Furthermore, the presence of spatial variation in P also leads to an additional energy component, known as gradient energy. This is because the magnitude of P in each FE unit cell is correlated to its strain and thus, the spatial variation in P (dP/dx, dP/dy and dP/dz) leads to another energy component that depends on the elastic coupling between the unit cells. This gradient energy density (f_{grad}) can be written as the following

equation [Eq. (2)]:

$$f_{grad} = g_{11}(\partial P/\partial x)^2 + g_{11}(\partial P/\partial y)^2 + g_{44}(\partial P/\partial z)^2.$$
 (2)

Therefore, the total energy density (f_{total}) in an FE layer can be written as 26,27

$$f_{total} = f_{free} + f_{elec} + f_{grad}$$

$$= \frac{1}{2}\alpha P^{2} + \frac{1}{4}\beta P^{4} + \frac{1}{6}\gamma P^{6} - E.P$$

$$+ g_{z} \left(\frac{\partial P}{\partial z}\right)^{2} + g_{x} \left(\frac{\partial P}{\partial x}\right)^{2} + g_{y} \left(\frac{\partial P}{\partial y}\right)^{2}.$$
(3)

Here, g_i is the gradient coefficients along the i=x, y, and z directions. Now, according to the Landau–Ginzburg–Devonshire (LGD) theory, the time (t) dependent Ginzburg Landau (TDGL) equation (in the Euler–Lagrange form) can be written as 26,27

$$E - \frac{1}{\Gamma} \times \frac{\partial P(r)}{\partial t} = \alpha P(r) + \beta P(r)^{3} + \gamma P(r)^{5} - g_{11} \frac{\partial^{2} P(r)}{\partial z^{2}} - g_{44} \frac{\partial^{2} P(r)}{\partial v^{2}}.$$
 (4)

Here, Γ is the viscosity coefficient and $r \equiv (x, y, z)$. Note that, Eq. (4) is derived for a uniaxial FE, in which the P direction is restricted only along the z axis. However, if the FE is multi-axial so that the P can be directed in all the x, y, and z directions, then all the P components (as vectors) along with their cross-coupled terms are required to be considered. While such considerations are indeed required for multi-axial FE, to keep the discussion of this paper uncomplicated, we only consider uniaxial FE. In addition, the FE properties also depend on the mechanical strain in the film. If such strain is homogeneous along the film thickness, then the strain contribution can be incorporated within the Landau coefficients (Ref. 40). We embraced such assumptions and thus the Landau coefficients in Eq. (4) are strain-dependent.

Furthermore, it is important to note that the total interface charge density, Q (or out-of-plane displacement field, D) of the FE layer incorporates both the contribution from spontaneous P as well as the background out-of-plane linear permittivity $(\varepsilon_{r,z})$. Therefore, $Q = \varepsilon_0 \varepsilon_z^{FE} E + P(E)$. At the same time, the presence of P variation causes the long-range Coulomb interaction leading to the in-plane electric fields in the FE layer. The associated energy with the in-plane electric field further depends on the in-plane background permittivity $(\varepsilon_x^{FE}$ and $\varepsilon_y^{FE})$. Therefore, to account for the associated energy with in-plane and out-of-plane electric fields in the background permittivity of the FE layer, Eq. (4) is needed to be solved self-consistently with Poisson's equation [Eq. (5)] as shown below:

$$-\varepsilon_0 \left[\frac{\partial}{\partial x} \left(\varepsilon_x^{FE} \frac{\partial \phi(r)}{\partial x} \right) + \frac{\partial}{\partial y} \left(\varepsilon_y^{FE} \frac{\partial \phi(r)}{\partial x} \right) + \frac{\partial}{\partial z} \left(\varepsilon_z \frac{\partial \phi(r)}{\partial z} \right) \right] = \frac{\partial P(r)}{\partial z}.$$
(5)

It is important to note that the P direction in FE can be altered (between -P and +P) by applying an electric field higher than the coercive field ($\pm Ec$). In this paper, we refer to such a change in the P direction as P switching. However, an applied electric field, less than the P switching field, can also change the P magnitude (without changing its direction), and we use the term "magnitude response" to refer to this aspect. Now, based on these discussed sets of equation [Eqs. (1)-(5)], let us discuss the possible mechanism of achieving NC effects in FE materials.

III. QUASI-STATIC NEGATIVE CAPACITANCE IN FERROELECTRIC HETEROSTRUCTURES

To stabilize a negative capacitor, a positive capacitor is required to be connected in series so that the total capacitance of the system remains positive. To explain this, let us consider a heterogeneous capacitive system comprising of a linear dielectric (DE) layer and an FE layer sandwiched between two metal electrodes. Such a system is also called metal-ferroelectric-insulator-metal (MFIM) stack [Fig. 2(a)]. Let us assume the individual (or separately measured) capacitance of the DE and FE layers are C_{DE} and C_{FE} , respectively. If these individual capacitances remain unchanged in the MFIM stack, then the total capacitance of this system can be calculated as $1/(1/C_{DE}+1/C_{FE})$. However, if the effective capacitance of the FE layer ($C_{FE,EFF} < 0$) is negative, then the actual (measured) capacitance of the system, $C_{FE-DE} > 1/(1/C_{DE}+1/C_{FE})$, as well as $C_{FE-DE} > C_{DE}$. Such an effect is known as capacitance enhancement effect and can be regarded as the signature of the negative capacitance (NC) effect of the FE layer. On the other hand, if $C_{FE-DE} > 1/(1/C_{DE}+1/C_{FE})$, but $C_{FE-DE} < C_{DE}$, that would

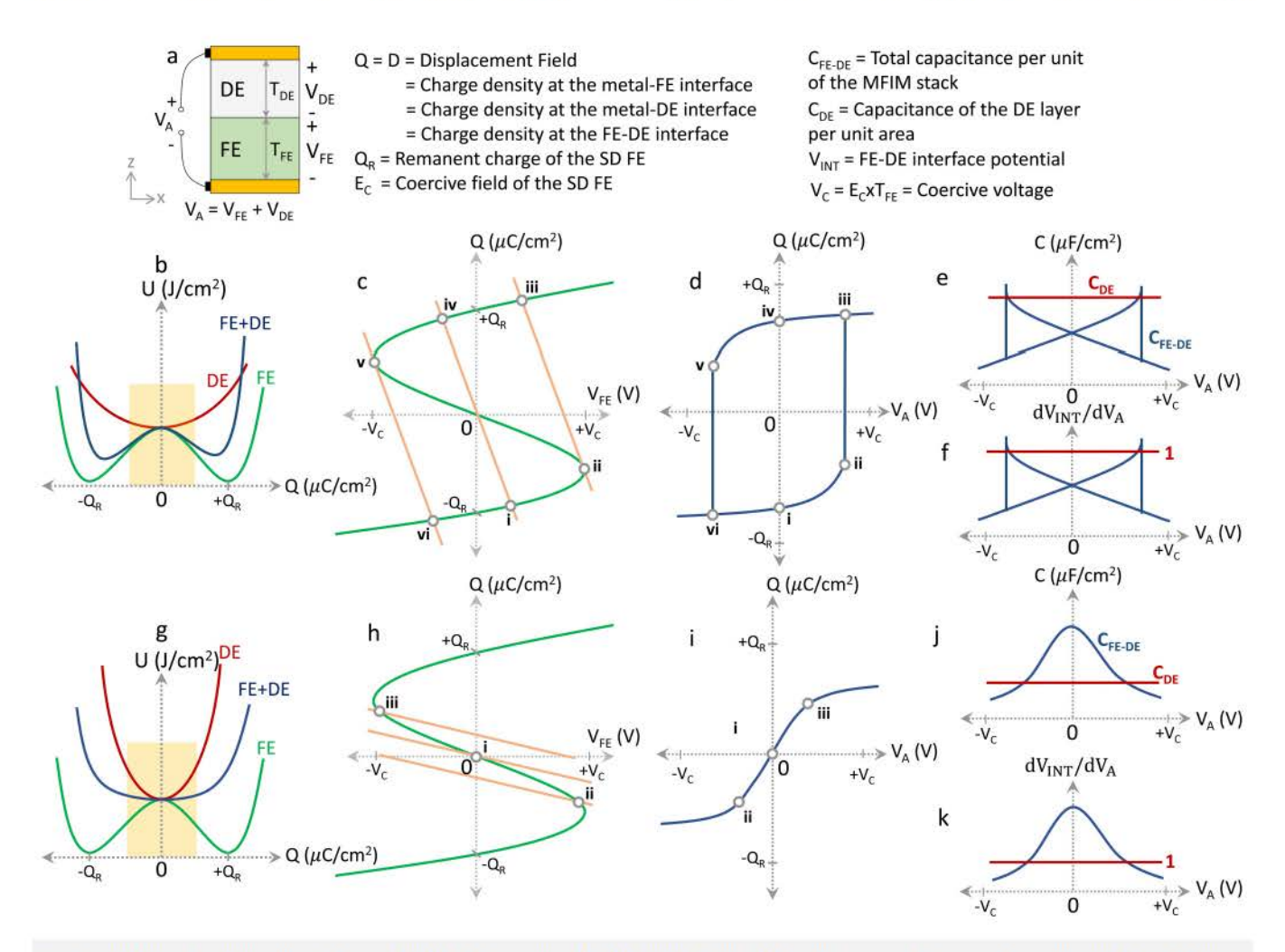


FIG. 2. (a) Metal–ferroelectric—dielectric—metal (MFIM) or ferroelectric (FE)–dielectric (DE) stack. Here, the FE layer is assumed to be in a single-domain state. Considering a low DE thickness (C_{DE} > min–|dQ/dV_{FE}| × T_{FE}) (b) Energy landscape (U–Q) of FE, DE and FE-DE stack, corresponding (c) Q–V_{FE} and load-line conditions, (d) Q–V_A characteristics, (e) C–V_A characteristics, and (f) dV_{NT}/dV_A characteristics. Considering a higher DE thickness (C_{DE} < min–|dQ/dV_{FE}| × T_{FE}) (g) energy landscape of FE, DE, and FE-DE stack, corresponding (h) Q–V_{FE} and load-line conditions, (i) Q–V_A characteristics, (j) C–V_A characteristics, and (k) dV_{INT}/dV_A characteristics.

imply the effective capacitance of the FE layer is higher than its standalone value $(C_{FE,EFF} > C_{FE})$ but not negative. Therefore, depending on the extent of enhancement, $C_{FE,DE} > 1/(1/C_{DE} + 1/C_{FE})$ can be observed either (1) due to an enhanced effective FE capacitance $(C_{FE,EFF} > C_{FE})$ or (2) due to the negative effective FE capacitance $(C_{FE,EFF} < C_{FE})$. While the latter effect is the so-called NC effect in FE, the former effect can also play an important role in FE based device operation (discussed later), and sometimes can be confused with the NC effect, if not analyzed properly.

Now, let us discuss the NC effect in FE in an MFIM stack. Depending on whether the FE layer is in a single-domain (SD) state or multi-domain (MD) state, the implication of the NC effect and the corresponding conditions to stabilize them are quite distinct. Therefore, in Sec. III A, we first discuss the stabilization of the NC effect in SD FE.

A. Negative capacitance effect in single-Domain FE

To impose the condition that the FE layer is in a single-domain (SD) state, let us assume that the gradient energy coefficient is infinite ($g_{11} = g_{44} \rightarrow \infty$). That implies that a non-zero spatial variation in P would lead to infinite gradient energy. Therefore, to minimize the energy, the P in the FE layer is restricted to be homogeneous (dP/dx = dP/dz = dP/dz = 0). In this hypothetical SD FE, the average polarization in FE is equal to its microscopic P and the free energy (U) landscape is as same as the microscopic free energy landscape (f_{free}) with respect to P. Similarly, by imposing dP/dx = dP/dz = dP/dz = 0 is Eq. (4), the P vs E relation can be written as $E-(1/\Gamma)$ ($\partial P/\partial t$) = $\alpha P + \beta P^3 + \gamma P^5$.

Now, considering a static scenario (dP/dt = 0), one can immediately see the presence of a region in its P-E characteristics that exhibit $dP/dV_{FE} < 0$ as well as the $dQ/dV_{FE} < 0$ region [see Fig. 2(b)]. Such a NC region (sometimes, referred to as the intrinsic negative capacitance region of FE7,12) is indeed unstable in a standalone MFM capacitor and, therefore, the corresponding charge response would be hysteretic. However, the NC region can potentially be stabilized in an MFIM stack [Fig. 2(a)]. The Q vs applied voltage (V_A) response of such a MFIM stack can be understood from the load line picture [shown in Fig. 2(c)] by considering the $Q-V_{FE}$ response of an FE layer with a thickness of T_{FE} and $Q-V_{DE}$ response of the DE layer. That suggests, if $C_{DE} > \min - |dQ|$ $dV_{FE}|\times T_{FE}$, then the NC region is unstable, and the corresponding $Q-V_A$ characteristics of the MFIM stack exhibits hysteresis [Fig. 2(d)]. However, the NC region can, in principle, be stabilized, if the DE capacitance $C_{DE} < \min - |dQ/dV_{FE}| \times T_{FE}$, and for that the corresponding $Q-V_A$ characteristics become non-hysteretic⁷ [Figs. 2(g)-2(i)]. In this case, the total capacitance of the MFIM stack, $C_{FE-DE} > C_{DE}$ since $C_{FE,EFF} < 0$ [Fig. 2(j)]. Consequently, the differential change in the FE-DE interface potential (VINT) with respect to applied voltage (VA) shows an amplified characteristic, $dV_{int}/dV_A = [1 + C_{FE,EFF}/C_{DE}]^{-1} > 1$ [Fig. 2(k)].

Now, to get a physical perspective of these phenomena, let us consider the implication of depolarization electric field in FE. In an FE material with finite thickness, the spontaneous *P* induced bound charge appears at its interface. If these bound charges are not compensated, then it should exert an electric-field which is opposite to the direction of *P* and hence called depolarization field.

Such a depolarization field causes an increase in the electrostatic energy in the FE layer called depolarization energy. However, in a metal-FE-metal (MFM) configuration with ideal metal electrodes, the metal can provide the compensating charge for the spontaneous P induced bound charge without any additional energy. Therefore, in an ideal scenario, the spontaneous P state (that corresponds to the minimum of the free energy) is stabilized in an MFM configuration and the P switching are hysteretic. However, in the MFIM stack, due to the presence of the DE layer in between the FE and metal layer, the P induced bound charge cannot be compensated immediately at its interface. Rather, the bound charge will produce an electric field in the DE layer and that electric field will eventually get compensated in the metal-DE interface. However, the electric field in the DE layer gives rise to a potential drop across the DE thickness. Considering the short-circuited scenario (or applied voltage, $V_A = 0$ V), an equal and opposite potential should appear across the FE thickness ($V_{FE} = -V_{DE}$) and that will lead to a depolarization field in the FE layer. In such a scenario, the depolarization field will lead to non-zero depolarization energy (-E.P). That would further lead to a reduction in the P magnitude leading to an increase in free energy and a decrease in depolarization energy so that the total energy of the system is minimized. In short, in the SD scenario, the depolarization field leads to an increase in free energy by homogeneously reducing the P magnitude [Fig. 2(c)]. However, if the DE layer is sufficiently thick (small C_{DE}), the depolarization field can be so high that the system prefers to climb the entire free energy barrier, fully suppressing the spontaneous P(P=0). In this scenario, the minimum energy configuration of the system is obtained by maximizing the free energy of the FE layer so that the depolarization energy of the FE and electrostatic energy of the DE layers is minimized. Therefore, at $V_A = 0 \text{ V}$, Q = 0 (as P = 0), $V_{FE} = 0$ (zero depolarization energy in FE), and $V_{DE} = 0$ (zero electrostatic energy in the DE). In other words, a significant amount of energy remains stored in the FE layer for obtaining the minimum energy configuration of the system.

Now, if a non-zero voltage is applied across the MFIM stack $(|V_A| > 0)$, it should lead to an increase in the charge density (Q) of the metal plates as well as the P magnitude of the FE layer. This results in a positive capacitance of the whole stack $(dQ/dV_A > 0)$ as well as the positive susceptibility of the FE layer with respect to the external voltage ($dP/dV_A > 0$). Interestingly, an increase in P magnitude (from P=0) implies a decrease in its free energy because of the double-well shaped free energy landscape of FE [Fig. 2(g)]. At the same time, the depolarization energy (-E.P) increases. However, within a certain region, the decrease in free energy is more compared to the increase in depolarization energy and thus, the total FE energy decreases with the increase in P magnitude. Therefore, the total energy in the DE layer is equal to the energy supplied by the external voltage source plus the decreased energy in the FE layer. In other words, the transfer of the energy from the FE layer to the DE layer leads to the enhanced energy of the DE beyond the energy supplied from the source. As a result, for the same V_A , the DE layer in MFIM can experience a higher displacement field compared to the situation when it is a stand-alone entity. A higher displacement field in the DE layer translates to a higher V_{DE} (> V_A) and that further leads to the differential amplification of V_{INT} $(dV_{\rm INT}/dV_A>1)$. Similarly, the charge response (dQ/dV_A) , which is the capacitance of the whole stack, increases beyond the value of the capacitance of the DE layer $(C_{FE-DE}>C_{DE})$. Such capacitance enhancement as well as the amplification of V_{INT} , which are the features of NC effect in FE, should take place within a specific operational region within which $d^2U/dQ^2<0$ so that total FE energy can decrease (decrease in free energy dominates over the increase in depolarization energy) with the change in Q.

Now, the condition for non-hysteretic operation can be understood from the perspective of the transfer of energy between FE and DE. For the hysteresis free operation, this energy transfer is required to be adiabatic. Such a condition is satisfied, if for a differential change in Q (dQ), the decrease in FE energy (dU) is less than the required energy of the DE layer to induce a similar charge. The differential change in energy of a capacitor can be written as $dU = Q \times (1/C) \times dQ$. From that, we can obtain the condition for obtaining non-hysteretic and quasi-static NC effect for FE in an MFIM stack to be $1/|C_{FE,EFF}| < 1/C_{DE}$ or $C_{DE} < |C_{FE,EFF}|$.

So far, our discussion was based on the assumption that the polarization in the FE layer is homogeneous across its thickness and area. However, in reality, the polarization can spatially vary both along with its thickness and in-plane directions because the gradient energy coefficient is indeed finite. Moreover, in the presence of the depolarization field, the formation of a multi-domain state in the FE layer is a likely possibility^{2–5,49,50} and such a multi-domain structure has a very important implication from the perspective of negative capacitance.^{2–5} To analyze that, next, we discuss the multi-domain formation in the MFIM stack and the corresponding NC effect in the multi-domain FE layer.

B. Negative capacitance effect in multi-domain FEs

Recall that in MFIM stack with the single-domain FE, the partial compensation of depolarization energy takes place by reducing the P magnitude and thus at the cost of the free energy [Fig. 3(a)].

However, for finite gradient energy coefficient (g), the ferroelectric has one more option to decrease the overall energy, i.e., break into multiple domains with opposite P directions. Indeed, in such a multi-domain (MD) state of the ferroelectric, the depolarization energy, as well as the increase in free energy, can be significantly suppressed [Fig. 3(b)]. In this scenario, the P induced bound charges at the FE-DE interface not only give rise to out-of-plane electric fields but also produce in-plane electric fields, called stray fields [Fig. 3(b)]. As the bound charges are partially getting compensated by the interfacial stray-field, it further reduces the constraint for the out-of-plane electric field in the FE and DE layers, leading to a lower depolarization field compared to the single-domain state. Consequently, this reduces the requirement for the increase of the local P magnitude, which reduces the free energy compared to the single-domain state. In other words, the MD state can suppress depolarization energy as well as free energy.

However, this suppression of free energy and depolarization energy takes place at the cost of some additional energy associated with the formation of domain-wall (the boundary between the domains with opposite P directions). One component of domainwall (DW) energy is the electrostatic energy associated with the interfacial stray field, and the other component is the gradient energy linked with the variation in P at the DW. As the formation of the MD state occurs as an interplay among competing energy components to obtain the minimum energy of the whole system, it is no wonder that the configuration of the MD state is strongly dependent on the DW energy. In Ref. 27, it has been shown that, depending on the DW energy, the types of DW can be either "hard" or "soft". Here, the term "hard" implies that the change in P direction is abrupt at the DW, and thus, the physical thickness of the DW is atomically thin [Figs. 4(b) and 4(c)]. In contrast, in "soft" DW, the change in P direction takes place by gradually changing its magnitude over the length scale of several unit cells [Figs. 4(d) and 4(e)]. In an FE with a certain thickness, the DW can be hard for small "g" and soft for a larger "g." The nature of

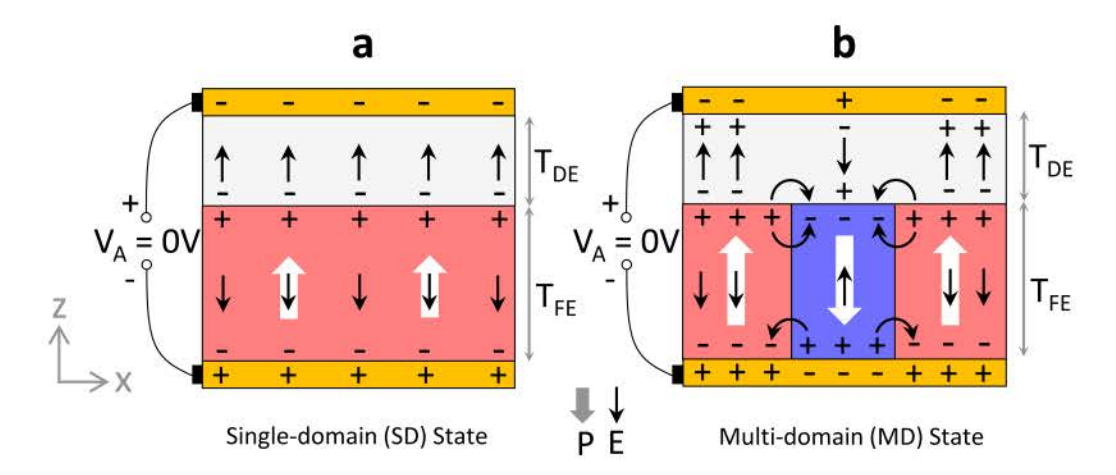


FIG. 3. MFIM stack with the FE layer in (a) single-domain (SD) state and (b) multi-domain (MD) state. In the SD state, minimum energy is obtained at cost of a significant increase in free energy by suppressing the local P magnitude. In the MD state, minimum energy is obtained in a cost of domain-wall (DW) energy where the average P decreases rather than local P.

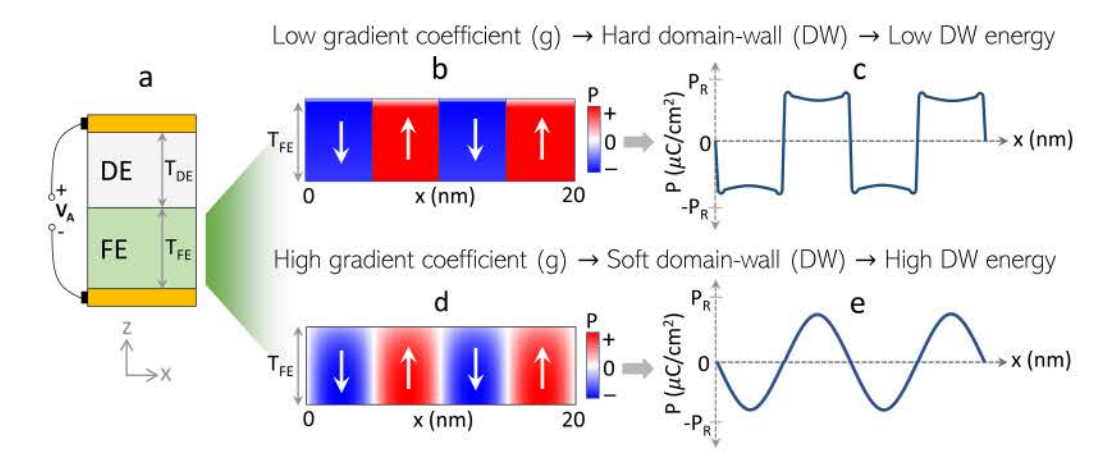


FIG. 4. (a) MFIM stack. (b) Multi-domain polarization configuration (b) with hard-DW where (c) the change in P direction occurs abruptly and (d) with soft-DW where (e) the change in P direction takes place with a gradual change in P magnitude.

the DW (hard or soft) plays an important role in the P switching characteristics of the FE layer. Before going to the discussion of P switching, it is noteworthy that in the MD state, Q, U, V_{FE} , and V_{DE} represent the average quantities. This is because of the spatial varying P in the MD state, which further leads to non-homogeneous potential, electric-field, and energy density profiles in the FE and DE layer.

Note that the DW energy (total of this gradient energy and the electrostatic energy) gives rise to higher local energy near the DW compared to the rest of the film. In hard-DW, this local DW energy density is lower than the maximum of the free energy barrier. Interestingly, in the MD state with hard-DW, Q = 0 state can be obtained with multiple equal size domains with opposite P directions. Consequently, the average energy (U) increases (due to the DW energy) but remains significantly lower compared to the SD scenario [Fig. 5(a)]. This is because in the SD state, Q = 0 can only be achieved by maximizing the free energy (local P = 0). While in the MD state, P is not required to be locally zero and can eventually remain close to its spontaneous value for which free energy is low. Furthermore, within the limit of MD state with hard-DW, Q=0 can be obtained with different domain periods [Fig. 5(a)]. As the average energy density (U) depends on the DW energy which further depends on the number on DWs, the maximum U that corresponds to Q = 0 is not unique [Fig. 5(a)]. Moreover, the domain period even depends on the physical thickness of the DE layer (i.e., the domain pattern becomes denser with the increase in DE and decrease in FE thickness). As a result, the average energy landscape (U-Q) of MD FE with hard-DW in the MFIM stack is not unique [Fig. 5(a)], which is a very distinct feature of the MD state compared to the SD state.

Since the local DW energy density in hard-DW is lower than the maximum of the free energy barrier, therefore, an additional energy is required to initiate the DW displacement. In other words, to obtain *P* switching for DW displacement, a voltage greater than a critical voltage must be applied to surpass the free energy barrier. As a result, the *P* switching characteristics in MD FE with

hard-DW displacement are hysteretic [Fig. 5(b)]. This implies that once the DW is displaced due to a certain V_A larger than a positive critical value, a reverse DW displacement will not occur just by reducing the V_A to zero. For that, V_A is required to be lower than another negative critical value. Furthermore, the DW displacement takes place in a discrete fashion (lattice by lattice) and each of these displacements corresponds to the overcoming of a local energy barrier. Such local barriers, as well as local minima, manifest in the average energy landscape of FE [Fig. 5(a)—yellow line]. Note that, different MD configurations with different average Q states corresponding to these local minimums can be stabilized at $V_A = 0$ V. Therefore, Q- V_A characteristics with hard-DW scenario are hysteretic and show a signature of partial P switching with different remanent charges [Fig. 5(b)].

Now let us turn our attention to MD FE with soft-DW. Note that the local DW energy density in the soft-DW is higher compared to the hard-DW due to higher "g" in the former. In fact, if the nature of DW is substantially soft, the local energy density in the DW becomes comparable to the maximum of the free energy density. In this case, an infinitesimally small differential increase in V_A would lead to the DW displacement. Furthermore, when V_A returns to zero, the DW displacement would seamlessly take place in the reverse direction and the FE will return to its equilibrium domain configuration. Therefore, the soft-DW displacement leads to adiabatically reversible P switching. Moreover, the P configuration in MD FE with soft-DW is unique and that leads to a unique average energy landscape [Fig. 5(d)]. As a result, the P switching as well as the corresponding Q– V_A characteristics are non-hysteretic [Fig. 5(e)].

It is remarkable that the DW displacement-based P switching in FE leads to an effective NC path in the $Q-V_{FE}$ characteristics in the MFIM stack, irrespective of the type of DW in FE. To understand that, first note that the electric-field in the FE layer is depolarizing due to the presence of the DE layer. This implies that in each of the domains, the local electric field is opposite to its P direction. Macroscopically, the DW displacement causes a change

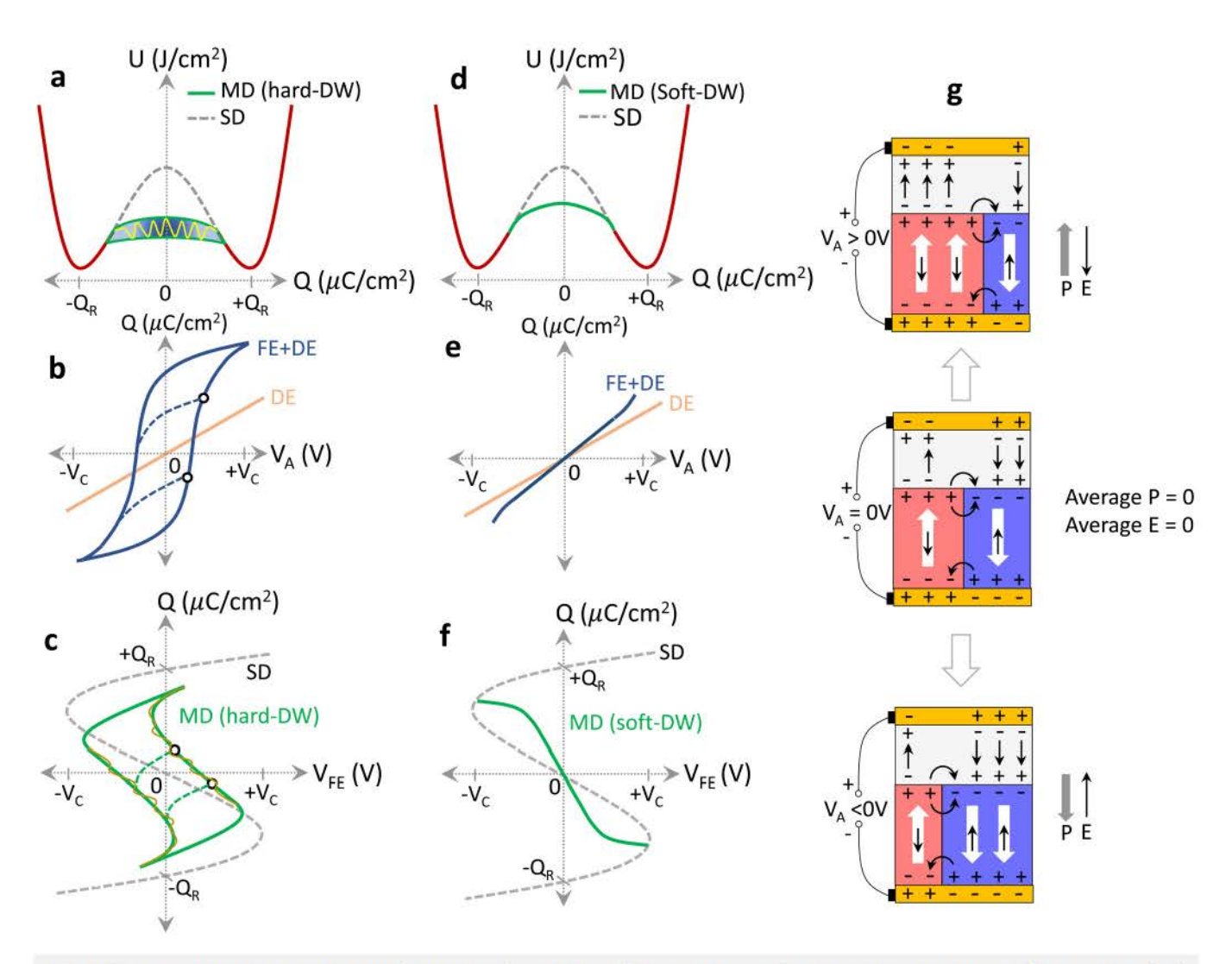


FIG. 5. Considering multi-domain FE with hard-DW (low DW energy) in MFIM stack: (a) energy landscape of FE where the shaded regions signify the possibilities of different multi-domain configurations with different average energy (U) for the same average charge density (Q), where $U=(1/A)\int (f_{free}+f_{grad})dV$ and A is the in-plane surface area of the FE film. The yellow line displays the presence of local minima and barriers associated with hard-DW displacement for achieving different average Q. Corresponding (b) $Q-V_A$ characteristics and (c) $Q-V_{FE}$ characteristics for a certain FE and DE thickness signifying partial polarization switching (minor loops—as different MD states with different Q can be stabilized at the same V_A) and hysteretic NC effect in FE. Here the zigzag nature of the P switching path corresponds to the yellow in (a). Considering multi-domain FE with soft-DW (high DW energy) in the MFIM stack: (a) energy landscape of FE which is unique for a certain FE thickness signifying a unique MD configuration. Corresponding (b) $Q-V_A$ characteristics and $Q-V_{FE}$ characteristics display non-hysteretic NC behavior. (g) Polarization and electric field profile in the MFIM stack for different V_A illustrating a generic scenario of DW displacement base P switching in FE and the macroscopic mechanism of NC effect as an outcome of increasing average P with an increasing depolarization field (opposite to the P direction).

in average polarization which further leads to an increase in the depolarizing field [Fig. 5(g)]. Such a depolarization field dominates the total field in the FE layer. As the increase in average polarization takes place simultaneously with the increase in depolarization field (which is opposite to the polarization direction), the effective capacitance of the FE layer becomes negative. $^{4,20,26,27}_{-20,20}$ Note that such a description of the FE NC effect does not require the concept of local P to be zero or the local free energy to be maximum.

Moreover, the displacement of a hard DW implies a sharp change in the P direction (due to lattice by lattice P switching). Therefore, the local P switching is not adiabatic and thus observed NC effect in Q- V_{FE} characteristics exhibits hysteresis. However, in the case of soft-DW displacement, the change in local P direction takes place by gradually changing its magnitude. Therefore, the local P switching for soft-DW displacement is adiabatic, which leads to the non-hysteretic NC effect. To get a clearer picture of the NC effect under

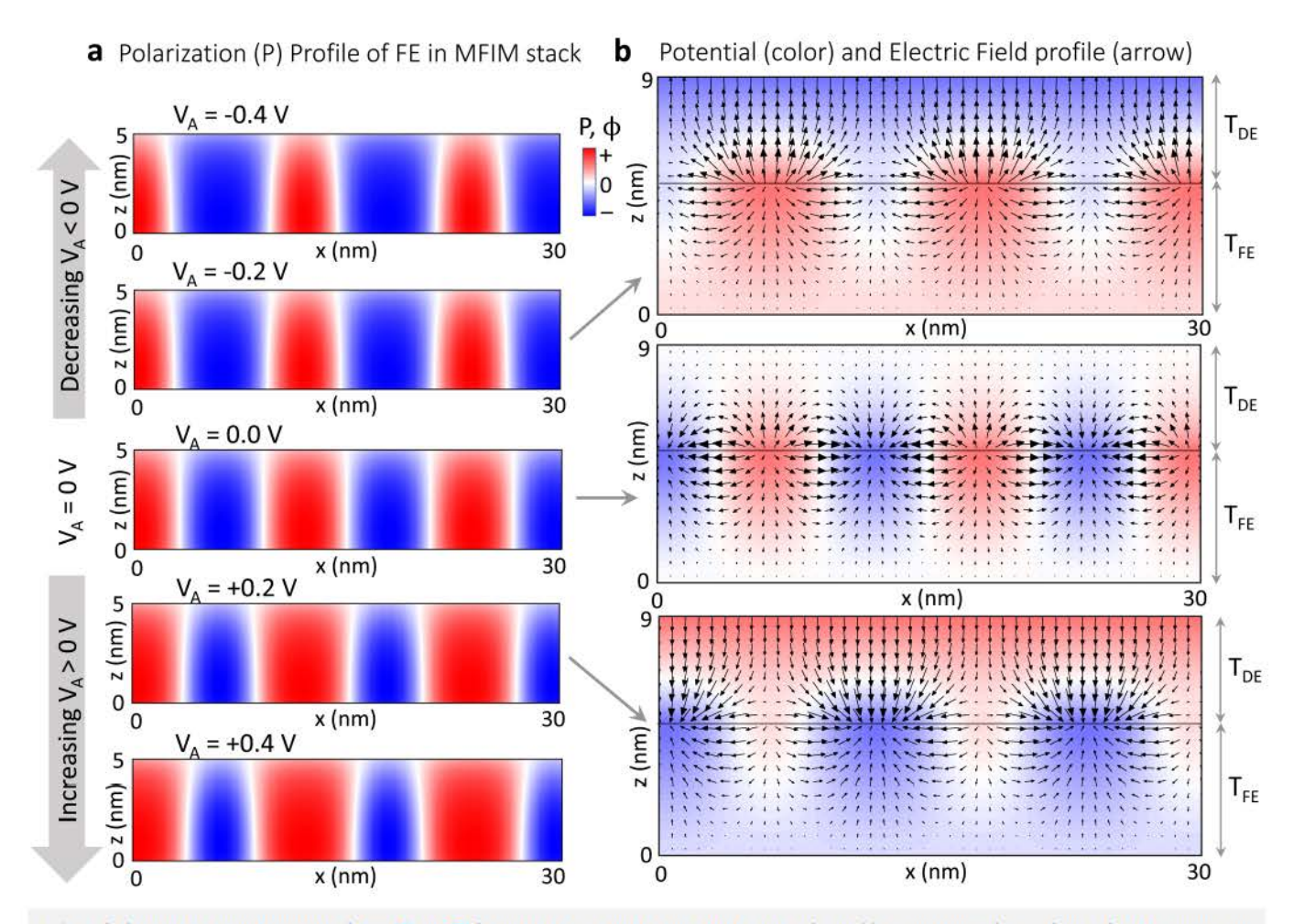


FIG. 6. Self-consistent simulation results of Eqs. (4) and (5) for an MFIM stack that includes MD FE with soft-DW. (a) Polarization profile signifying soft-DW displacement-based P switching and corresponding (b) potential profile and electric field profile in the FE and DE layers. The potential profile signifies non-homogeneous interface potential. The electric field profiles display the redistribution of the interfacial stray field due to DW displacement.

soft-DW displacement, in addition to the macroscopic features (increasing average *P* with increasing depolarization field), it is important to capture the microscopic phenomena (Fig. 6). Microscopically, the soft-DW displacements (i) redistribute the interfacial stray fields and (ii) decrease the DW energy resulting in a negative net contribution to the total FE energy.^{23,27} This leads to a local effective negative capacitance within the FE layer^{13,23,25,27} primarily near the FE-DE interface [due to the stray field redistribution, see Fig. 6(b)] and the DW (due to decrease in DW energy).

Furthermore, it is important to note that, even though the effective NC path (negative dQ/V_{FE} region) of MD FE with soft-DW is non-hysteretic, it is quite different from the SD NC path [Fig. 5(f)]. In fact, the MD NC effect is lower compared to SD FE [Fig. 5(f)]. This is because the average energy in the MD state is lower compared to the SD state [Fig. 5(d)]. Thus, the reduction in energy (dU) for the same change in charge density (dQ) will be higher in SD FE compared to MD FE. Therefore, $1/|C_{SD,EFF}^{SD}|$ >

 $1/|C_{FE,EFF}^{MD}|$ (Note: a higher NC effect implies a larger $1/|C_{FE,EFF}^{SD}|$). Moreover, it is noteworthy that the MD NC path depends on the permittivity of the DE layer because of the dependency of electrostatic DW energy (due to stray field) on the in-plane permittivity of the DE layer. It has been shown that the FE NC effect enhances for the lower in-plane permittivity of the DE layer. This provides an interesting distinction between the MD NC and SD NC phenomena. However, within the soft-DW limit, the MD NC path should not depend on the physical thickness of the DE layer as long as the DE thickness is sufficient enough to accommodate the interfacial stray fields.

Now, let us discuss the capacitance enhancement effect in the MFIM stack for MD NC. As the NC effect with soft-DW is non-hysteretic, a conventional C-V measurement will inevitably reveal an enhanced capacitance of the MFIM stack compared to its DE counterpart ($C_{FE-DE} > C_{DE}$). However, due to the involvement of hysteresis associated with the hard-DW displacement, the situation

becomes somewhat non-trivial as the NC effect is not seamlessly reversible. In a small signal C-V measurement, if the peak-to-peak value of the applied small-signal voltage (V_{PP}) is not sufficient to surpass the local barrier to induce the DW displacement, then the NC effect may not be observed. However, if V_{PP} is sufficiently high to induce the DW displacement, then it may be possible to observe NC effect and hence, the C-V measurement should signify $C_{FE-DE} > C_{DE}$.

Now, recall that the internal potential (V_{INT}) is homogeneous for SD FE which exhibits a differential amplification $(dV_{INT}/dV_A>0)$ due to the SD NC effect. However, in the case of MD FE, V_{INT} is non-homogeneous and it spatially varies by following the polarization profile in the FE layer. ^{26,27} Moreover, V_{INT} exhibits spatially local maxima and minima corresponding to +P and -P domains, respectively. Nevertheless, the MD NC effect provides a differential amplification to the average V_{INT} , but the extent of amplification is spatially non-homogeneous. ²⁷ This is another important distinction between the SD NC and MD NC effects.

C. Correlation between FE thickness and NC effect

So far, we have discussed the possibilities of different types of NC effect (SD-NC, MD-NC with soft and hard-DW) in FE depending on the value of gradient coefficients signifying the importance of having a higher "g" for obtaining non-hysteretic NC effect via SD-NC or MD-NC with soft-DW. However, since "g" is a material parameter, it may be challenging to tune it with device optimization to meet the design requirements. (This needs further investigation, e.g., by analyzing the effect of strain via metal contacts on g, which might provide a design knob to control g, albeit only to a certain extent). Therefore, a relevant question to ask is if the nature of the DWs can be controlled by a device design parameter. To that end, the utilization of an interesting correlation between the physical thickness and the MD state in the FE layer has been proposed in Refs. 27 and 28.

According to the Landau–Kittle formula 49,50 ($W \propto \sqrt{T_{FE}}$), the domain width (W) in an isolated FE slab (in MD state with 180° DW) is proportional to the square-root of the FE thickness (T_{FE}). Therefore, with the decrease in physical thickness, the domain pattern in the FE layer becomes denser [Figs. 7(a) and 7(b)]. Based on a more extensive simulation for FE-DE stack, a similar correlation was obtained in Refs. 26–28 [Fig. 7(c)]. With the scaling of FE thickness, as the domain pattern becomes denser, the type of DW makes a transition from hard to soft type 27,28 and by scaling T_{FE} further the SD state can potentially be stabilized [Figs. 7(b)–7(d)]. However, such critical T_{FE} for the (i) hard-DW to soft-DW transition ($T_{FE,MD-soft}$) and as well as MD state to SD state transition ($T_{FE,SD}$) depends on the value of gradient coefficient (g). In Ref. 27,

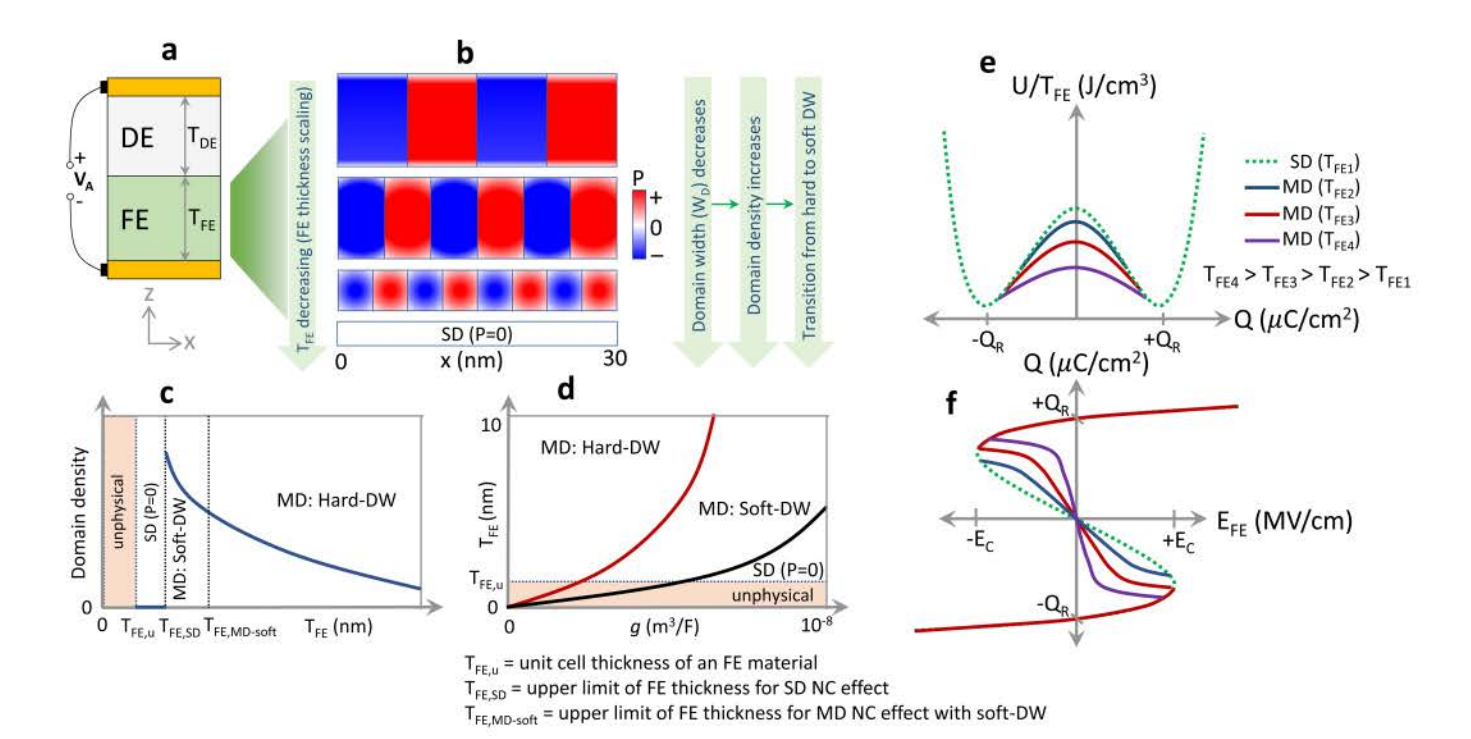


FIG. 7. (a) MFIM stack, (b) MD polarization configuration signifies that the domain density increases and the type of DW make a transition from hard to soft with the decrease in FE thickness. (c) Dependency between the domain density and FE thickness signifying that stability of (i) MD state with hard-DW for $T_{FE} > T_{FE,MD-soft}$ (ii) MD state with soft DW for $T_{FE,SD} < T_{FE} < T_{FE,MD-soft}$ and (iii) SD state for $T_{FE,SD} < T_{FE}$. (d) The conditions for MD states with hard/soft-DW and SD states for different g and T_{FE} . Here, the shaded region corresponds to FE thickness less than a unit cell, which is not physically realizable. (e) The energy density per unit FE thickness (U/T_{FE}) for different T_{FE} . (f) $Q-E_{FE}$ ($E_{FE} = V_{FE}/T_{FE}$) characteristics for different T_{FE} suggesting that the NC effect enhances with the decrease in FE thickness.

Saha *et al.* showed that the smaller "g" leads to a decrease in critical T_{FE} ($T_{FE,SD}$ and $T_{FE,MD-soft}$) as shown in Fig. 7(d). If "g" is so small that the critical T_{FE} becomes smaller than the thickness of an FE unit cell, then the FE layer may not be physically realizable. Therefore, for obtaining the non-hysteretic NC effect in FE, while FE thickness scaling is the key; however, at the same time, choosing an FE material with a considerably high gradient energy coefficients is an important design consideration. We will come back to this aspect in Sec. VII.

Provided that "g" is sufficiently large for achieving the MD state with soft-DW at a physically realizable T_{FE} , there further exists an interesting correlation between the effective permittivity [eff- $\varepsilon_z^{FE} = T_{FE} \times (\mathrm{d}Q/\mathrm{d}V_{FE})$] of the FE layer and the FE thickness. In Ref. 27, the author shows that the MD NC effect enhances (1/eff- ε_z^{FE} increases) and moves toward the SD NC path with the decrease in T_{FE} [Fig. 7(f)]. This is because, as the domain density in FE increases with T_{FE} scaling, the contribution of DW energy in the total FE energy increases. Therefore, the energy landscape of MD FE makes a gradual transition toward the energy landscape of SD FE with the decrease in T_{FE} [Fig. 7(e)]. As a result, the MD NC effect changes toward the SD NC effect with T_{FE} scaling.

It is important to note that the DW displacement is essential to obtain the NC effect in MD FE. However, there is another interesting phenomenon specific to hard-DW and in the absence of their displacement, which may be mistaken for non-hysteretic NC effect and therefore, is important to discuss here. This phenomenon occurs if the applied voltage is not sufficient to switch the P direction (so, no DW displacement). In this case, the $Q-V_A$ characteristics reflect the response of background permittivity of FE and the change in P magnitude (but not the direction) to the applied voltage and therefore, are non-hysteretic. At the same time, the effective permittivity of the FE layer shows an enhancement compared to its intrinsic value.²⁸ However, this permittivity enhancement cannot be due to the NC effect (as no P switching occurs), but rather is an electrostatic-driven phenomenon due to the MD state. In other words, the FE permittivity can enhance in the absence of DW displacement but remains positive which we will now discuss.

IV. ENHANCED BUT POSITIVE EFFECTIVE PERMITTIVITY OF FE IN THE MD STATE

Let us consider an MFIM stack [Fig. 8(a)] in which the FE layer is in the MD state with hard-DW and applied voltage (V_A) is insignificant to induce a change in the P direction (no DW displacement) [Figs. 8(b)–8(d)]. In such a scenario, the magnitude response of the local P with respect to the applied electric field and the associated redistribution of in-plane fringing fields in the FE layer (near the DW) is important to consider. In Ref. 28, the authors show that an applied voltage induced change in P magnitude leads to a conversion from in-plane to the out-of-plane electric field [Figs. 8(e)–8(g)]. Such a transformation of the electric-field direction leads to an additional charge in the FE–DE interface [Fig. 8(h)]. In other words, the stored electrostatic energy in the form of an in-plane electric field in MD FE gets transformed to and hence, provides a boost to the energy associated with the out-of-plane

displacement field [Figs. 8(e)-8(h)]. This leads to an increase in the charges on the metal electrode (those due to initial out-of-plane fields plus those by virtue of the transformed fields) and hence provides an enhancement in the effective permittivity of the FE layer.

Furthermore, this positive effective permittivity of FE ($\varepsilon_z^{FE} > 0$) is a function of its physical thickness [Fig. 8(i)]. This is because, (i) the in-plane stray fields (transformed to the out of plane fields on the application of voltage) and therefore, the associated additional charge at the FE-DE interface, appears near the DW and (ii) the domain density, as well as the DW density, increases with the decrease in FE thickness (as discussed before in Sec. III C). Therefore, the density of this additional charge increases with T_{FE} scaling. Consequently, ε_z^{FE} increases with the decrease in T_{FE} [Fig. 8(i)]. Also, it is noteworthy that this enhancement in the effective permittivity of MD FE28 is beyond the scope of the previous analytical equations 4,8,26 that capture the contribution of DW displacement. This is because in that formulation the magnitude response of P was neglected and the DW contribution was calculated based on their non-zero displacement. On the contrary, in Ref. 28, the enhanced effective permittivity is captured by selfconsistently considering the finite magnitude response P along with the T_{FE} -dependent MD configurations.

So far, we have discussed various possible mechanisms for the quasi-static NC effect where the FE NC region is stabilized in MFIM stacks, which further leads to quasi-static enhancement in capacitance. Now, to complete the picture, let us briefly turn our attention to yet another phenomenon which leads to the NC behavior in FE due to the transient effects.

V. TRANSIENT NEGATIVE CAPACITANCE EFFECT

The transient NC effect was first demonstrated by Khan et al. in a series-connected network of a resistor (R) and FE capacitor as shown in Fig. 9(a). They showed that when a positive voltage pulse was applied in an R-FE network [Fig. 9(b)], in the way of charging the FE capacitor (dQ > 0), the voltage drop across the FE capacitor decreases (dV_{FE} <0) for a short time period [Fig. 9(b)]. According to the single-domain LK model, the FE capacitor can be modeled as a series-connected constant resistor (R_{FE}) and a capacitor (C_{FE}) [Fig. 9(c)], where C_{FE} exhibits an intrinsic NC region [Fig. 9(d)]. In Ref. 12, the authors argued that the observed decreasing FE voltage while charging the FE capacitor (dQ/ dV_{FE} <0) can be understood as the signature of the intrinsic SD NC path of the FE layer. However, alternate explanations exist in the literature. 14,17,18 The work in Ref. 19 showed that such dQ/ dV_{FE} <0 can be described by the intrinsic delay associated with the P switching in the FE. In this work, the FE capacitor has been considered as a positive non-linear capacitor ($C_{FE} > 0$, which is described by the Miller model 19) connected in series with a resistor $(R_{FE} = \tau/C_{FE})$ that captures the delay (τ) associated with the domain nucleation and their subsequent growth. When the voltage pulse is applied at the R-FE network, the initial C_{FE} is small and R_{FE} is large. Thus, V_{FE} becomes larger than V_{CFE} due to the potential drop across R_{FE} [Fig. 9(e)], which can be regarded as "voltage overshoot". Near the coercive voltage, when P switching initiates, C_{FE} experiences a substantial increase yielding a large decrease in R_{FE} . As a result, the potential drop across R_{FE} decreases leading to

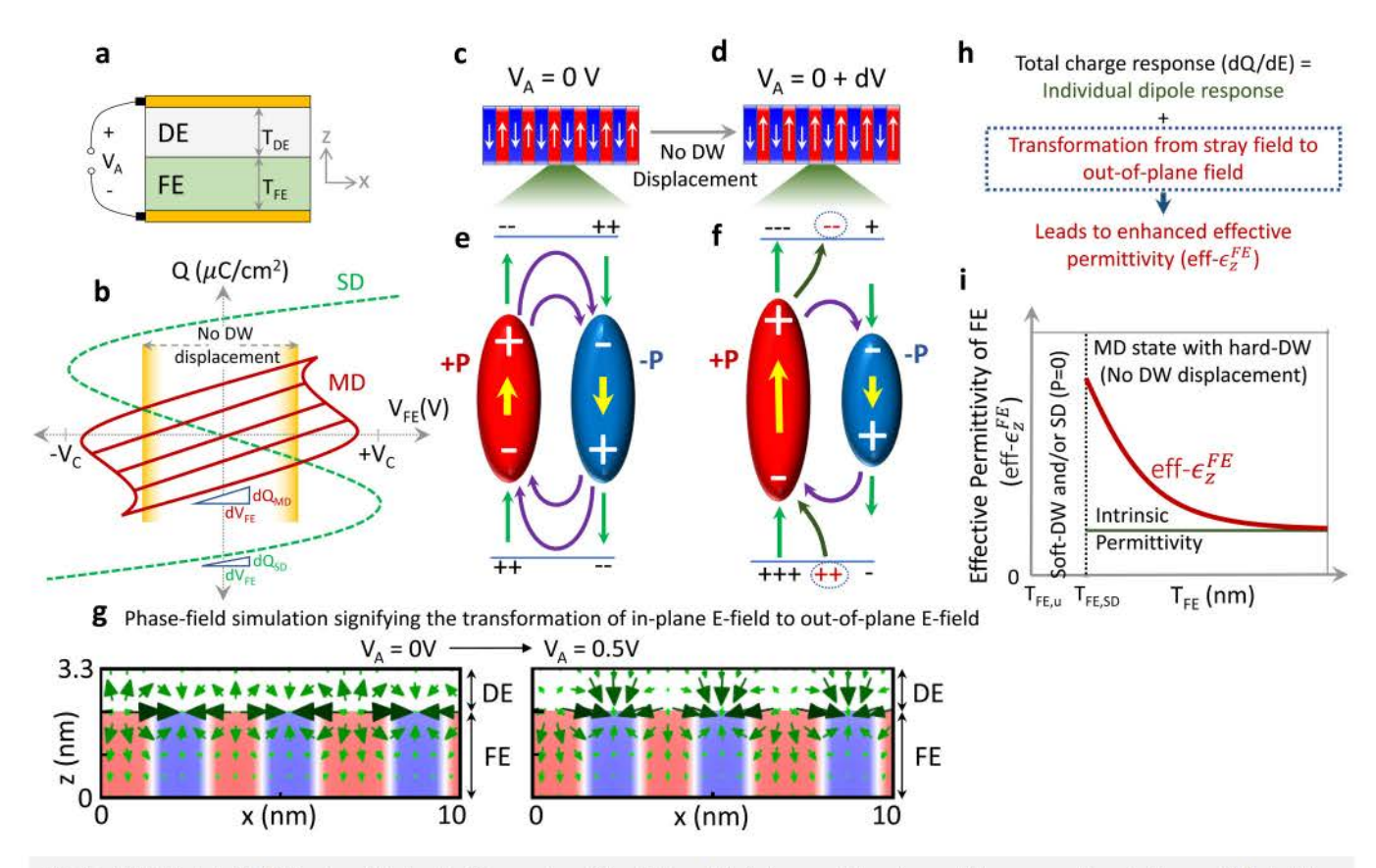


FIG. 8. (a) MFIM stack. (b) $Q-V_{FE}$ characteristics signifying a region within which no DW displacement takes place and the corresponding effective permittivity is higher than its intrinsic value. (c)–(f) A two dipole model and (g) phase-field simulation results (polarization: color, electric-field: vector) signifying the applied voltage driven directional change in electric-field at the FE-DE interface (adapted from Ref. 28). (h) Such transformation of the in-plane electric field to an out-of-plane electric field component leads to the enhancement in effective permittivity of the FE layer. (g) Phase-field simulation results (polarization: color, electric-field: vector) of MFIM stack with hard-DW signifying the directional change in electric-field at the FE-DE interface. (adapted from Ref. 28) (i) Dependency between effective FE permittivity and T_{FE} . Note that, if $T_{FE} < T_{FE,SD}$ then the DW becomes soft and thus small differential voltage would cause DW displacement leading to NC effect (eff $-\epsilon_Z^{\rm FE} < 0$).

an overall decrease in V_{FE} [Fig. 9(e)—snapback]. As a result, a larger current is obtained by enhancing the potential drop across the external resistor $(V_R = V_A - V_{FE})$ to support the charging of large C_{FE} . In such a situation, V_{CFE} is still increasing and hence, $C_{FE} = dQ/dV_{CFE} > 0$. Hence, during the charging/discharging of the FE capacitor, a negative dQ/dV_{FE} may appear as an artifact of V_{FE} overshoot and its subsequent snap-back. 19 Furthermore, this paper¹⁹ compares different trends by considering both the SD NC and apparent NC and provides guidelines to reveal the true origin of the transient NC effect. Similarly, the transient NC phenomenon has been analyzed in Refs. 14 and 17 based on the traditional domain switching model of the Kolmogorov-Avrami-Ishibashi (KAI) formalism, which explains the P switching in FE based on the nucleation and growth of reverse domains. According to their analysis,17 the decreasing voltage could be described by the mismatch between the influx of charge flow and its consumption by the reverse domain formation in the FE capacitor.

It is noteworthy that the quasi-static and transient NC effects, although related, may involve different physical mechanisms and therefore, the observation of one may not directly prove the existence of the other. As the focus of this paper is the quasi-static NC effect (which is directly related to NC-based device applications), we now discuss some of the experimental results on the NC effect and their correlation with the different types of mechanisms we have discussed so far.

VI. EXPERIMENTAL EVIDENCE OF NC EFFECT

The capacitance enhancement in FE-DE heterostructures, as a signature of NC effect in FE, has been first demonstrated by Khan et al. using PbZr_{0.2}Ti_{0.8}O₃ as the FE and SrTiO₃ as the DE layer. Beyond a critical temperature, the authors show that $C_{FE-DE} > C_{DE}$, which can be considered as an indication of negative effective C_{FE} in the heterostructure. Later, in 2014, Gao et al. demonstrated a similar effect¹¹ in FE-DE superlattice systems with LaAlO₃ as the DE material and Ba_{0.8}Sr_{0.2}TiO₃ as the FE materials. In both of the works, he should be picture of the NC effect has been implicitly adopted to justify the experimentally observed phenomena. However,

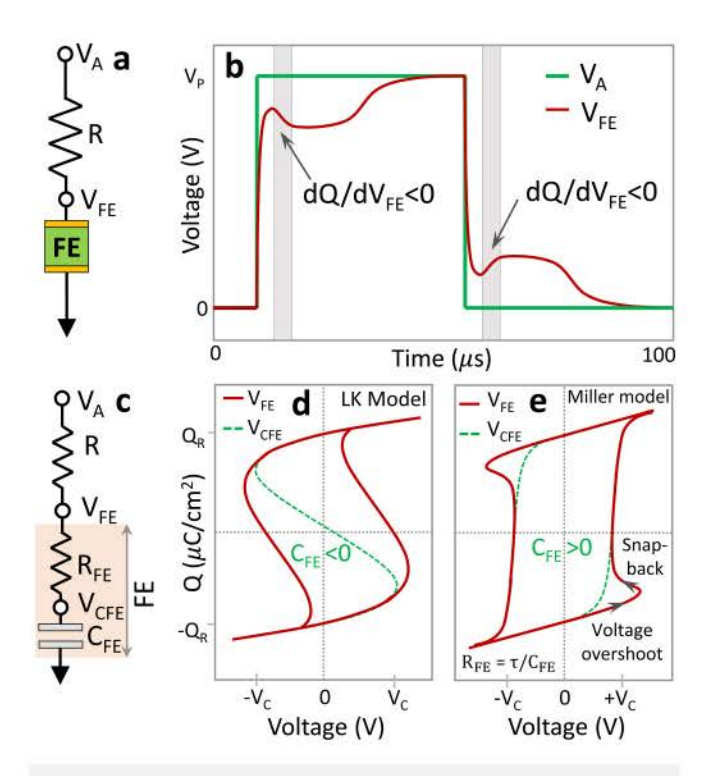


FIG. 9. (a) Schematic of a series-connected resistor (R) and ferroelectric (FE) capacitor network. (b) Transient response of the voltage across the FE layer (V_{FE}) upon the application of voltage pulses (V_A) across the R-FE network signifying a region with $dQ/dV_{FE} < 0$ in the charging/discharging response of the FE capacitor. Here, $dQ/dV_{FE} < 0$ represents the transient NC effect (c) Representative schematic model of R-FE network, where the FE capacitor comprises a series-connected resistive element (R_{FE}) and capacitive element (C_{FE}). $Q-V_{FE}$ and $Q-V_{CFE}$ characteristics based on (d) Landau–Khalathikov model suggesting that the negative dQ/dV_{FE} originates from intrinsically negative C_{FE} and (e) Miller model suggesting that negative dQ/dV_{FE} may originate even with a positive C_{FE} .

due to the absence of completely non-hysteretic *C-V* characteristics, the MD NC with hard-DW displacement can be regarded as a more reasonable mechanism. In 2016, P. Zubko *et al.* demonstrated a similar capacitance enhancement effect¹³ in an FE-DE superlattice (Pb_{0.5}Sr_{0.5}TiO₃-SrRuO₃) system for a wide range of temperatures and for the first time, such effect has been attributed to the MD NC effects in FE.¹³ Furthermore, in 2019, more extensive experimental measurements on PbTiO₃/SrTiO₃ superlattice, Yadav *et al.* mapped out the local effective permittivity of the FE layer signifying the presence of local negative effective permittivity near the FE-DE interface and DW.²⁵ Therefore, the presence of MD NC in perovskite FE can be regarded as a well-demonstrated concept. However, further investigation is required to justify whether the DWs are soft or not. To that effect, an experimental demonstration of non-hysteretic *Q-V* characteristics is yet to be demonstrated.

Recently, the NC effect in fluorite FE has been investigated by Hoffman *et al.* by considering an FE-DE heterostructure with Hf_{0.5}Zr_{0.5}O₂ as the FE and Ta₂O₅ as the DE layers. ⁵¹ Based on the applied voltage-pulse modulated charging of the FE-DE stack, the

authors traced out an S-shaped Q-VFE characteristics of the FE layer. In this work, 51 the author assumed that the depolarization field in the FE layer, which would appear due to the presence of the DE layer, is suppressed because of the presence of polarization compensating trap charges at the FE-DE interface. Based on this assumption, they argued that the FE layer is stabilized in the SD state rather than creating MD states. Therefore, according to the author, the experimentally observed S-shaped Q-VFE characteristics is a direct representation of the SD NC path which was also argued to be non-hysteretic. However, based on the same experimental data, Kittl et al. have shown that the actual trajectories of these Q-V characteristics exhibit hysteretic characteristics when both charging and discharging paths are considered.⁵² As we have already discussed that the hysteretic NC path is a feature of P switching in MD FE with hard-DW, therefore, the experimental result in Ref. 51 is neither a validation of hysteresis free SD NC path, nor a representation of the true nature of the Landau's double-well free-energy landscape in FE HfO2. While the presence of quasi-static NC effect (with or without hysteresis) is an indication of having a double-well energy landscape, a direct experimental evidence of SD NC effect is yet to be demonstrated.

Furthermore, as both the MD NC with soft-DW and SD NC is expected to be hysteresis free and exhibit similar macroscopic NC attributes, therefore, a direct experimental demonstration of SD NC requires to be focused on their microscopic distinction with MD NC. One of the possible mechanisms could be STEM imaging of the atomic configuration (similar to Ref. 25) in the FE layer to discard the presence of domain-walls or multi-domain states. Such an approach is certainly applicable for the perovskite FE material because of their detectable DW25 either by visualizing the different orientations in atomic displacement in different domains or by identifying the misfit strain near the DW. Note that in perovskites (ABO₃ crystals), both B and O atoms are spontaneously displaced, and the position of B atoms is generally detectable in STEM image. However, for FE HfO2 where oxygens are the only atoms that are spontaneously displaced, access to similar features is challenging. This is because of the negligible misfit strain near the DW and the very limited detectability of the position of oxygen atoms for their small atomic size. As a result, microscopic evidence of SD NC in HfO2 needs further experimental investigation. However, such challenges can possibly be overcome by considering the polarizationstrain correlation in FE materials. Note the unit cell size of FE HfO₂ can be determined from the STEM image and from there the change in cell size (strain) in response to applied voltage can also be detectable. In FE materials, out-of-plain strain (ε_{33}) is proportional to the square of its out-of-plane polarization (P). Therefore, a typical MFM capacitor exhibits a hysteretic butterfly-shaped strain-voltage relationship [Fig. 10(b)] by following the hysteretic polarization-voltage characteristics [Fig. 10(a)].

However, if an FE unit cell is stabilized at the P=0 of the S-shaped path [in Fig. 10(a)] then the corresponding strain of that FE unit cell would follow the U-shaped curve [in Fig. 10(b)]. Now, in the MFIM stack, if the FE layer is in the SD NC state then at $V_A=0$ V, the polarization is stabilized homogeneously at P=0. Therefore, a small change in V_A , irrespective of increase or decrease (from $V_A=0$), would lead to an increase in strain (due to U-shaped FE strain characteristic) homogeneously across the entire FE layer

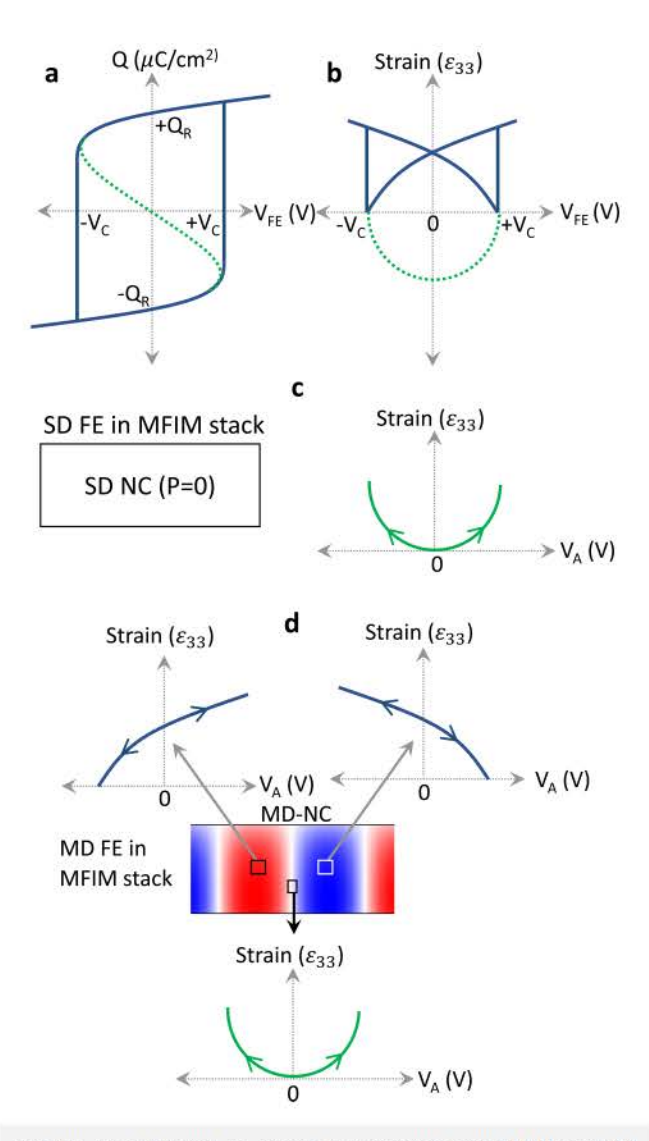


FIG. 10. (a) polarization vs voltage characteristics of the MFM capacitor showing hysteretic characteristics (blue line). The green line represents the unstable NC region. Corresponding (b) FE strain (ε_{33}) vs applied voltage characteristics of the MFM capacitor (blue line). The U-shaped dashed line corresponds to the S-shaped region in (a), which is unstable in the MFM capacitor. However, if the S-shaped region in $P\text{-}V_{FE}$ characteristics is stabilized in MFIM, then the U-shaped characteristics can also be obtained for ε_{33} – V_A characteristics. (c) In case of the SD NC effect, such U-shaped strain characteristics can be observed in the entire FE layer. (b) For the MD NC effect, the strain in the domains will follow the different branches of the butterfly curve and the DW will follow the U-shaped curve.

[Fig. 10(c)]. On the other hand, if the FE layer is in MD state, then the strain characteristic of the +P and -P domains will follow the two different branches of the butterfly curve as shown in Fig. 10(d). However, in the MD state, the local P=0 can be stabilized at the soft-DW and therefore, the U shape strain characteristics can only be observed at the DW [Fig. 10(d)]. Therefore, depending on whether

the U-shaped strain characteristics are observed throughout or only in a portion of the FE layer in the MFIM stack such an experiment can potentially reveal the true nature of the NC effect.

VII. MATERIAL PERSPECTIVE OF THE QUASI-STATIC NC EFFECT

As we have discussed that the stabilization of the NC effect in FE is strongly correlated to its elastic properties, therefore, it will be important to analyze this aspect from the perspective of different types of FE materials (i.e., perovskites and fluorite). The elastic coupling between neighboring unit cells can be determined from the dispersion of the polar phonon bands. For PbTiO₃, the curvature of these polar phonon bands is quite significant, which suggests a strong elastic coupling among the neighboring unit cells. Such strong elastic coupling further implies a high gradient energy coefficient (g) and thus the DW energy should be significantly large. This holds true for almost all the perovskite FE (i.e., PZT, BFO, etc.). Recall that the high DW energy is favorable for obtaining a non-hysteretic NC effect. Therefore, perovskite FE materials may be suitable for obtaining hysteresis free NC effects (either MD-NC with soft-DW or SD-NC).

In contrast, Lee et al. show that the polar phonon dispersion in fluorite FE (i.e., doped HfO2) is significantly small.53 Such a flat phonon band indicates a very low elastic interaction between fluorite unit cells. This is because of the presence of non-polar half-cell between the consecutive polar half-cells. As a result, the gradient coefficient (g) in the fluorite FE is expected to be very low so that the DW energy is negligible. For orthorhombic HfO2, it was shown that the DW energy is eventually negative,⁵³ which implies an anti-parallel configuration with 180° DW is more stable compared to a parallel configuration. Where this negative DW energy originates because of the (i) energy lowering due to the local compensation of P induced bound charge and (ii) insignificant DW energy. Considering this negligible DW energy, the MD formation in FE HfO2 is expected to be more prominent (for suppressing the depolarization field in an FE-DE stack) and even an MD state with the domain-width of a unit cell is not unlikely. Similarly, due to this negligible DW energy, achieving soft-DW as well as SD state in FE HfO2 is not very trivial. Therefore, for hysteresis free NC operation in FE HfO2, aggressive scaling of the FE thickness is essential. For example, it has been speculated that the MD-NC with soft-DW can be achieved in Zr doped HfO2 below the physical thickness of 1.5 nm.2

In short, the perovskite FE materials are more likely to provide quasi-static and hysteresis-free NC effect compared to the fluorite FE materials (i.e., doped HfO₂). On the other hand, from the perspective of CMOS process compatibility, the fluorite FE is a better choice compared to the perovskite FE. Therefore, material level optimizations, possibly by strain engineering and appropriate dopant selection, are required to harness hysteresis free NC effect in the fluorite FE family. At the same time, exploration of other FE materials (i.e., multi-ferroics, 2D ferroelectrics) featuring high elastic coupling as well as CMOS compatibility can lead to new opportunities for the future possibilities of the FE NC effects in integrated electronic devices.

VII. IMPLICATION OF DIFFERENT NC MECHANISMS IN FEFETS

While in this article, we mainly focus on NC phenomena in MFIM stack, evaluating its implication in the gate stack of FEFETs requires a similar analysis for a metal-ferroelectric-insulator-semiconductor (MFIS) stack. Such an analysis has been conducted in Ref. 27 by considering MD NC with soft-DW. It has been shown that similar to the MFIM stack, the MD NC effect leads to charge and capacitance enhancement as well as internal voltage amplification in the MFIS stack.27 However, in the MD scenario, the nonhomogeneous internal potential leads to a significantly nonhomogeneous potential profile at the semiconductor surface, which is quite distinctive compared to the SD NC effect. A quantitative analysis on the implication of such potential non-homogeneity in the electronic transport of FEFET has not yet been investigated. Nevertheless, to complete the discussion on NC attributes, next, we provide a qualitative perspective on the implication of different mechanisms of NC effect on the FEFET characteristics.

In conventional metal-oxide-semiconductor FET [MOSFET as shown in Fig. 11(a)-11(b)], only a fractional change in applied gate voltage (V_{GS}) appears as the change in semiconductor surface potential (Ψ) due to a voltage drop across the positive gate dielectric capacitance and therefore, $d\Psi/dV_{GS}$ < 1. Consequently, in the drain current (I_D) vs gate voltage (V_{GS}) characteristics of MOSFET, the attainable sub-threshold swing $[SS = dV_{GS}/dlog_{10}(I_D)]$ is always higher than 60 mV/decade at room temperature (300 K). However, we discussed that the FE layer in the gate stack of FEFET [Fig. 11(c)] can act as an effective negative capacitor under certain conditions. Such negative capacitance effects can provide differential amplification of the interface potential $(d\Psi/dV_{GS} > 1)$, which can potentially lead to steep-slope behavior (SS < 60 mV/decade) in the I_D - V_{GS} characteristics of FEFET, as predicted by the SD NC effect or as expected from the MD soft-DW induced NC effect 26,27 [see Fig. 11(d)]. In addition to the steep-slope characteristics, FEFET also exhibits several unique features directly correlated with the NC phenomena in FE. One of such features is negative output conductance (NOC) which is also known as negative differential resistance (NDR) observed in the I_D - V_{DS} characteristics of FEFETs in their ON state.18 While in conventional MOSFETs, the output conductance is positive, FEFETs can exhibit negative output conductance due to the effective NC effect of the FE layer in the gate stack. A similar effect is negative drain-induced barrier lowering (N-DIBL), 18 which is associated with the drain voltage-dependence of NC effect in the OFF state of the FEFET. To explain these V_{DS} dependent effects, let us first explain the impact of V_{DS} on I_D . An increase in V_{DS} leads to two primary effects: (i) it increases the lateral electric field in the semiconductor channel which tends to increase the I_D and (ii) it alters the source barrier and the electric fields in the gate oxide. The latter effect can also be thought of as capacitive coupling between the drain and gate oxide capacitances. In the case of conventional MOSFETs, the gate oxide capacitance is positive and hence, the increase in V_{DS} leads to an increase in surface potential. In the typical I_D - V_{DS} characteristics, the former effect leads to a linear increase in I_D that saturates at a certain V_{DS} . However, the saturation current $(I_{D,SAT})$ keeps increasing due to the latter effect as the surface potential increases with the increase in

 V_{DS} . Therefore, the output conductance $(g_{DS} = dI_{D,SAT}/dV_{DS})$ of conventional MOSFET is always a positive quantity. However, in FEFET, if the FE layer acts as an effective negative capacitor, then the increase in V_{DS} can potentially lead to a decrease in average potential at the interface of the ferroelectric and dielectric in the gate stack (V_{INT}) . This is because as V_{DS} increases, the drain capacitance tends to reduce the electric displacement in the dielectric and the ferroelectric layers. (Note, this effect, in general, is more on the drain side, but also penetrates on the source side due to electrostatic coupling and domain interactions, as discussed later.) In response to the decrease in electric displacement, the electric fields in the FE must increase since the FE capacitance is negative. For a fixed gate voltage, this is possible when V_{INT} reduces. To sum up, if $C_{FE} < 0$, increase in V_{DS} can have two opposing effect of I_D due to increase in lateral electric field (which tends to increase I_D) and V_{INT} reduction (which tends to reduce I_D). Therefore, the I_D - V_{DS} curve of FEFET can exhibit a region where I_D decreases with the increase in V_{DS} when V_{INT} reduction dominates. This occurs when V_{DS} is sufficiently high that the effect of the lateral electric field diminishes. This reduction in I_D with V_{DS} yields negative output conductance (NOC) or negative differential resistance (NDR)18,54 in the output characteristics of FEFETs [see Fig. 11(e)]. Similarly, when the FEFET is OFF, similar effect occurs, which leads to negative DIBL $(N-DIBL)^{18,54}$ as shown in Fig. 11(e). In other words, when V_{DS} increases, the drain electric field lines reduce the polarization and electric displacement in the FE layer. This reduces V_{INT} and pulls up the source barrier leading to N-DIBL. While the above description provides a macroscopic understanding of the NC phenomena responsible for reduced SS, NOC (or NDR) and N-DIBL in FEFETs, the microscopic nature of the NC effect plays an important role and is thus required to be understood properly.

Recall our earlier discussion that the nature of the NC effect in FE depends on the value of its gradient energy coefficient, g. Also, for certain FE thickness, there exists a lower limit for g above which the FE layer can potentially exhibit SD NC effect. Note that the SD NC effect in MFIM/MFIS stack implies a homogeneous polarization profile along the lateral dimensions. However, the nonhomogeneous potential distribution in the FE layer of the FEFETs (due to the source and drain regions) leads to a non-uniform electric-field in the FE layer along the gate length direction. 18 This leads to a mild non-homogeneity in polarization, even in the SD NC regime with finite g. Considering such polarization nonhomogeneity in the SD NC regime, it has been shown that the NC attributes of FEFET enhance with the increase in g. In other words, the NC related FEFET properties, i.e., reduction in SS, N-DIBL and NOC are maximum when $g = \infty$ (homogeneous polarization profile) and decreases with the decrease in g. This suggests that the domain interactions in the FE layer play a key role in transmitting the effect of V_{DS} from the part of the FE layer in proximity to the drain to that closer to the source. As a result, larger domain coupling (g) in FE offers lower SS, higher N-DIBL and higher NOC in FEFET characteristics.11

Now, recall that if g is lower than a critical value, then the formation of the MD state takes place in the FE layer. In such a scenario, depending on the value of g, the nature of the FE DW can be either soft or hard (as discussed earlier). Similar to the SD NC effect, the MD NC effect with soft DW should also provide

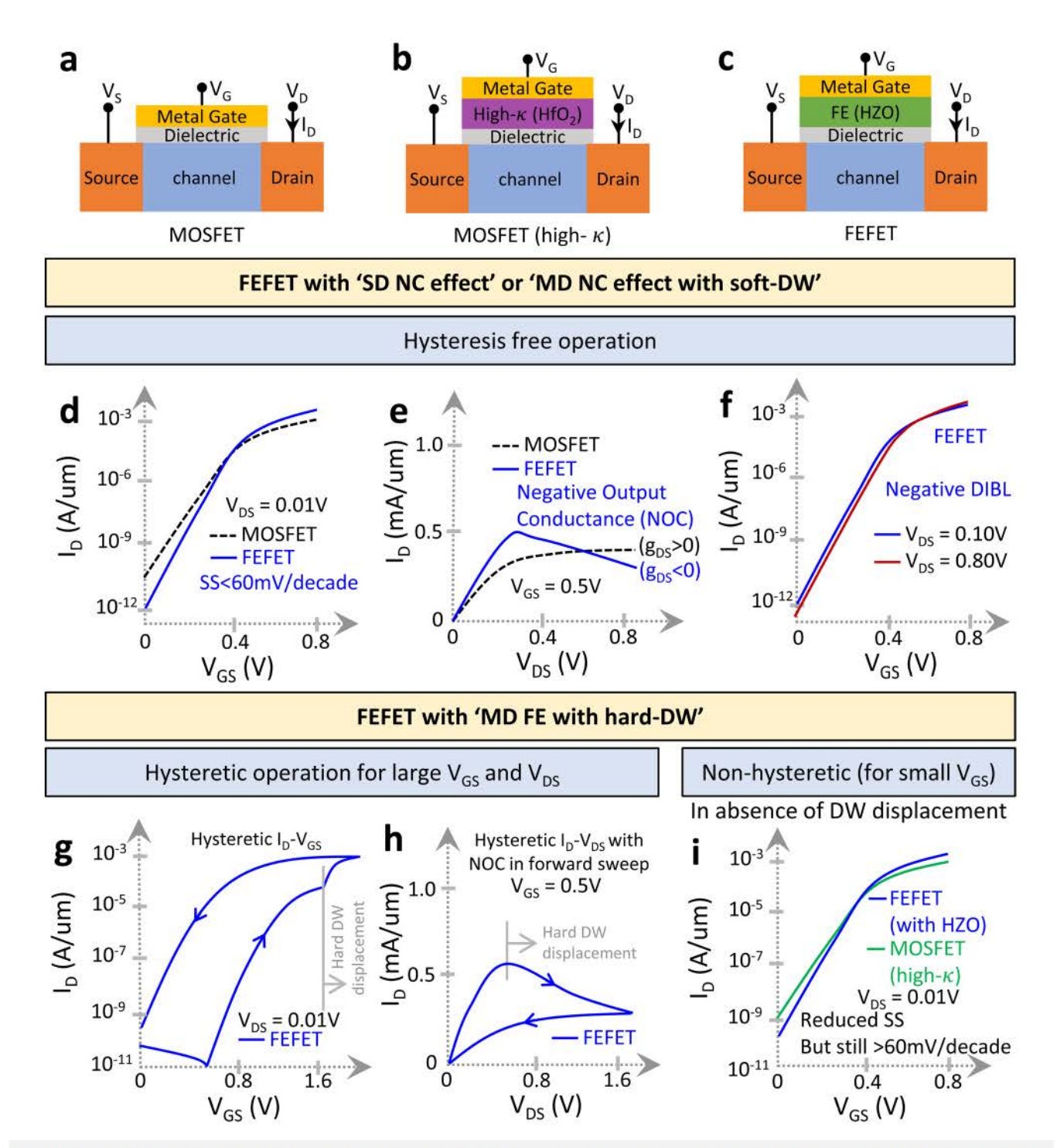


FIG. 11. Physical structures of (a) conventional MOSFET, (b) MOSFET with high-k gate oxide (i.e. HfO_2), and (c) Ferroelectric FET (FEFET). (d)–(f) FEFET characteristics with the FE layer exhibiting SD NC effect or MD NC effect with soft-DW displacement signifying (d) steep-slope (SS < 60 mV/decade), (e) negative output conductance (NOC), and (f) negative-DIBL characteristics. In this case, the device operation in non-hysteretic. (g)–(h) FEFET characteristics with the FE layer exhibiting MD NC effect with hard-DW displacement signifying (g) hysteretic I_D – V_{GS} and (h) hysteretic I_D – V_{DS} characteristics. (i) In the MD FE with hard-DW, if the applied V_{GS} is not sufficient to cause polarization switching (i.e., DW displacement), then hysteresis free I_D – V_{GS} characteristics can be obtained exhibiting enhanced permittivity or high-k operation in FEFET with HZO as gate oxide (compared to the HfO₂ based high-k MOSFET).

SS < 60 mV/decade, negative-DIBL and NOC in FEFET characteristics. However, such attributes are expected to be less prominent for MD NC compared to the SD NC due to the reduced NC effect in the former case.²⁷ Furthermore, considering the correlation between the MD NC effect with soft-DW and g (MD NC effect decreases with the decrease in g), it can also be expected that the reduction in SS, negative-DIBL and NOC should decrease with the decrease in g. Note that, both of the SD NC effect and MD NC effect with soft-DW are non-hysteretic and hence, the SS, DIBL and output-conductance characteristics of FEFET should be hysteresis free with respect to the V_{GS} and V_{DS} sweep directions. It is noteworthy that the FEFETs featuring non-hysteretic steep-slope behavior are also familiar as negative capacitance FET (NCFET) and are suitable candidate for low power logic devices due to the possibilities of aggressive voltage scaling without sacrificing the drive current.

However, if the FE layer is in MD state with hard DW (low g), then the process of polarization switching (i.e., DW displacement) is non-adiabatic, leading to hysteretic NC effect. Hence, SS < 60 mV/ decade can be observed but exhibits hysteresis in the SS vs VGS characteristics. Due to the presence of hysteresis in the I_D - V_{GS} characteristics, such devices are suitable candidates for non-volatile memory operations²⁸ [Fig. 11(g)]. In addition, by modulating the amplitude of applied V_{GS} , different extent of partial polarization switching in FE can be obtained yielding different I_D at the same static bias conditions in FEFET. Based on this working principle, hysteretic FEFETs with MD FE have been investigated as the potential candidate as multi-level synapses for neuromorphic hardware. 45 Now, let us discuss the implication of hard-DW displacement in the I_D - V_{DS} characteristics. For a certain V_{GS} , if the drain voltage V_{DS} increases beyond a critical point (typically $V_{DS} > V_{GS}$), then partial polarization switching (+P to - P) takes place near the drain side of the FE layer. This leads to a decrease in channel potential and hence, an increase in barrier height for electron transport near the drain side of the channel, which decreases the drain current. Therefore, a decreasing ID with increasing V_{DS} (or NOC) can be observed in FEFET during the forward V_{DS} sweep given that the maximum V_{DS} is sufficient to cause the polarization switching in the FE layer [Fig. 11(h)]. However, during the reverse V_{DS} sweep (when V_{DS} returns to 0 V), the polarization configuration of the FE layer is retained (due to the hard nature of the DW). As a result, I_D - V_{DS} characteristics follow a different reverse path compared to its forward path. Moreover, due to the absence of polarization switching, NOC would not be observed in reverse V_{DS} sweep [Fig. 11(h)]. Concisely, in FEFET exhibiting hard-DW displacement, the I_D - V_{DS} characteristics are hysteretic and the NOC should typically be observed only in the forward V_{DS} sweep as shown in earlier works both theoretically and experimentally. Note that, the NOC mechanism for MD NC with hard-DW displacement (due to polarization switching induced drain side barrier enhancement) is quite distinct compared to the NOC mechanism we discussed for SD NC scenario where the effect of drain side polarization change influences the source side polarization due to finite domain-coupling and thus, modulates the energy barrier near the source side of the channel.

In the above discussion of FEFET employing MD FE with hard-DW, we assume that the applied V_{GS} and V_{DS} is sufficient to

cause hard-DW displacement and that further yields the negative effective permittivity of the FE layer. However, if the applied V_{GS} and V_{DS} are not sufficient to cause the DW displacement, then the device characteristics should be hysteresis free. Furthermore, in the absence of DW displacement, the effective permittivity of the MD FE with dense domain patterns is positive but is higher than its intrinsic value²⁸ (discussed in Sec. IV). Consequently, the FEEET with MD FE in the absence of DW displacement should display all the attributes of a FET with a high-k gate dielectric. That implies FEFET with HZO as FE layer with a thickness that corresponds to MD state with hard-DW should exhibit reduced SS (but still greater than 60 mV/decade) and reduced short channel effect (lower output conductance and lower DIBL) compared to a FET in which the FE layer is replaced with HfO2 layer having same physical thickness [see Fig. 11(i)]. Such a device is also suitable for low power logic devices as discussed in Ref. 28.

To complete the discussion, recall that *g* in perovskite materials is expected to be sufficiently large for obtaining hysteresis free NC and hence, FEFETs employing perovskite FE with a properly optimized thickness are more likely (compared to fluorite FE) to exhibit non-hysteretic steep-slope, NOC, and N-DIBL characteristics.

VII. SUMMARY

We discussed the possible mechanisms of the origin of negative capacitance behavior of ferroelectric materials in MFIM heterostructures based on the Landau-Ginzburg-Devonshire formalism. By discussing the implication of elastic coupling between ferroelectric unit cells, we examined the implication of the negative capacitance effect in the single-domain and multi-domain scenarios. While single-domain NC or intrinsic NC effect may take place for significantly large gradient energy coefficient, the multidomain NC effect is more probable for the realistic values of gradient coefficient, especially for fluorite structures. In MD FE, even though the nature of the NC effect can be quasi-static, the presence of hysteresis further depends on the nature of DW. The MD NC effect due to hard-DW displacement exhibits hysteretic characteristics, while for soft-DW displacement, a hysteresis-free NC effect can be obtained. Moreover, we discussed different features of the MD NC effect, in particular, the dependency of the effective negative permittivity of the FE layer on its physical thickness as well as the properties of the underlying dielectric materials. Due to such dependency, the MD NC effect should not be believed as an intrinsic effect, rather can be considered as an effective phenomenon. Moreover, we discuss the possible mechanism for obtaining the MD state with soft-DW by FE thickness scaling. In addition, we emphasize that, under certain scenarios, the effective permittivity of the FE layer may not be negative but can exhibit a higher effective permittivity compared to its intrinsic value. Such phenomena occur in the absence of DW displacement in MD FE with hard-DW due to the electrostatic interaction between domains. In addition, we review the relevant experimental demonstration of the FE NC effect and discussed their correlation with different types of NC mechanisms. Finally, we provide a brief perspective on the perovskite and fluorite based FE materials from the viewpoint of hysteresis free NC effects and their possible applications in electronic devices.

DATA AVAILABILITY

The data that support the findings of this study are available from the corresponding author upon reasonable request.

ACKNOWLEDGMENTS

This work was supported by the Semiconductor Research Corporation (SRC) under Contract No. 2020-LM-2959 and the National Science Foundation (NSF) under the Grant No. 1814756.

REFERENCES

- ¹R. Landauer, "Can capacitance be negative?," Collect. Phenom. 2, 167-170 (1976). ²A. K. Jonscher, "The physical origin of negative capacitance," J. Chem. Soc. Faraday Trans. 2(82), 75 (1986).
- ³A. Kopal, P. Mokrý, J. Fousek, and T. Bahník, "Displacements of 180° domain walls in electroded ferroelectric single crystals: The effect of surface layers on restoring force," Ferroelectrics 223, 127-134 (1999).
- ⁴A. M. Bratkovsky and A. P. Levanyuk, "Very large dielectric response of thin ferroelectric films with the dead layers," Phys. Rev. B 63, 2-5 (2001).
- ⁵A. M. Bratkovsky and A. P. Levanyuk, "Depolarizing field and 'real' hysteresis loops in nanometer-scale ferroelectric films," Appl. Phys. Lett. 89, 253108 (2006).
- ⁶I. Ponomareva, L. Bellaiche, and R. Resta, "Dielectric anomalies in ferroelectric nanostructures," Phys. Rev. Lett. 99, 227601 (2007).
- ⁷S. Salahuddin and S. Datta, "Use of negative capacitance to provide voltage amplification for low power nanoscale devices," Nano Lett. 8, 405-410 (2008).
- ⁸A. Cano and D. Jiménez, "Multidomain ferroelectricity as a limiting factor for voltage amplification in ferroelectric field-effect transistors," Appl. Phys. Lett. 97, 133509-12 (2010).
- ⁹A. I. Khan, D. Bhowmik, P. Yu, S. J. Kim, X. Pan, R. Ramesh, and S. Salahuddin, "Experimental evidence of ferroelectric negative capacitance in nanoscale heterostructures," Appl. Phys. Lett. 99, 113501 (2011).
- ¹⁰D. J. R. Appleby, N. K. Ponon, K. S. K. Kwa, B. Zou, P. K. Petrov, T. Wang, N. M. Alford, and A. O'Neill, "Experimental observation of negative capacitance in ferroelectrics at room temperature," Nano Lett. 14, 3864-3868 (2014).
- 11W. Gao, A. Khan, X. Marti, C. Nelson, C. Serrao, J. Ravichandran, R. Ramesh, and S. Salahuddin, "Room-temperature negative capacitance in a ferroelectricdielectric superlattice heterostructure," Nano Lett. 14, 5814-5819 (2014).
- ¹²A. I. Khan, K. Chatterjee, B. Wang, S. Drapcho, L. You, C. Serrao, S. R. Bakaul, R. Ramesh, and S. Salahuddin, "Negative capacitance in a ferroelectric capacitor," Nat. Mater. 14, 182-186 (2015).
- ¹³P. Zubko, J. C. Wojdeł, M. Hadjimichael, S. Fernandez-Pena, A. Sené, I. Luk'yanchuk, J.-M. Triscone, and J. Íñiguez, "Negative capacitance in multidomain ferroelectric superlattices," Nature 534, 524-528 (2016).
- ¹⁴S. J. Song, Y. J. Kim, M. H. Park, Y. H. Lee, H. J. Kim, T. Moon, K. D. Kim, J.-H. Choi, Z. Chen, A. Jian, and C. S. Hwang, "Alternative interpretations for decreasing voltage with increasing charge in ferroelectric capacitors," Sci. Rep. 6, 1-6 (2016).
- 15Y. J. Kim, M. H. Park, Y. H. Lee, H. J. Kim, W. Jeon, T. Moon, K. D. Kim, D. S. Jeong, H. Yamada, and C. S. Hwang, "Frustration of negative capacitance in Al₂O₃/BaTiO₃ bilayer structure," Sci. Rep. 6, 19039 (2016).

 16Y. J. Kim, H. Yamada, T. Moon, Y. J. Kwon, C. H. An, H. J. Kim, K. D. Kim,
- Y. H. Lee, S. D. Hyun, M. N. H. Park, and C. S. Hwang, "Time-dependent negative capacitance effects in Al₂O₃/BaTiO₃ bilayers," Nano Lett. 16, 4375-4381 (2016).

 17Y. J. Kim, H. W. Park, S. D. Hyun, H. J. Kim, K. D. Kim, Y. H. Lee,
- T. Moon, Y. B. Lee, M. H. Park, and C. S. Hwang, "Voltage drop in a ferroelectric single layer capacitor by retarded domain nucleation," Nano Lett. 17, 7796–7802 (2017).

 18 A. K. Saha, P. Sharma, I. Dabo, S. Datta, and S. Gupta, "Ferroelectric transistor
- model based on self-consistent solution of 2D Poisson's, non-equilibrium Green's function and multi-domain Landau Khalatnikov equations," in

- International Electron Devices Meeting (IEDM) (IEEE, San Francisco, CA, 2017),
- pp. 13.5.1–13.5.4. ¹⁹A. K. Saha, S. Datta, S, and S. K. Gupta, "Negative capacitance" in resistorferroelectric and ferroelectric-dielectric networks: Apparent or intrinsic?," . Appl. Phys. 123, 105102 (2018).
- ²⁰I. Luk'yanchuk, A. Sené, and V. M. Vinokur, "Electrodynamics of ferroelectric films with negative capacitance," Phys. Rev. B 98, 024107 (2018).
- ²¹M. Hoffmann, A. I. Khan, C. Serrao, Z. Lu, S. Salahuddin, M. Pešić, S. Slesazeck, U. Schroeder, and T. Mikolajick, "Ferroelectric negative capacitance
- domain dynamics," J. Appl. Phys. 123, 184101 (2018).

 ²²M. Hoffmann, M. Pesic, S. Slesazeck, U. Schroeder, and T. Mikolajick, "On the stabilization of ferroelectric negative capacitance in nanoscale devices," Nanoscale 10, 10891-10899 (2018).
- ²³J. Íñiguez, P. Zubko, I. Luk'yanchuk, and A. Cano, "Ferroelectric negative capacitance," Nat. Rev. Mater. 4, 243-256 (2019).

 241. Luk'yanchuk, Y. Tikhonov, A. Sené, A. Razumnaya, and V. M. Vinokur,
- "Harnessing ferroelectric domains for negative capacitance," Commun. Phys. 2, 22 (2019).
- ²⁵A. K. Yadav, K. X. Nguyen, Z. Hong, P. García-Fernández, P. Aguado-Puente, C. T. Nelson, S. Das, B. Prasad, D. Kwon, S. Cheema, A. I. Khan, C. Hu, J. Íñiguez, J. Junquera, L.-Q. Chen, D. A. Muller, R. Ramesh, and S. Salahuddin, "Spatially resolved steady-state negative capacitance," Nature 565, 468-471 (2019).
- ²⁶H. W. Park, J. Roh, Y. B. Lee, and C. S. Hwang, "Modeling of negative capacitance in ferroelectric thin films," Adv. Mater. 31, 1805266 (2019).
- ²⁷A. K. Saha and S. K. Gupta, "Multi-domain negative capacitance effects in metal-ferroelectric-insulator-semiconductor/metal stacks: A phase-field simulation based study," Sci. Rep. 10(1), 1-12 (2020).
- 28 A. K. Saha, M. Si, K. Ni, S. Datta, P. D. Ye, and S. K. Gupta, "Ferroelectric thickness dependent domain interactions in FEFETs for memory and logic: A phase-field model based analysis," in IEEE International Electron Devices Meeting (IEDM) (IEEE, San Francisco, CA, 2020), pp. 4.3.1-4.3.4.
- ²⁹J. Müller, T. S. Böscke, U. Schröder, S. Mueller, D. Bräuhaus, U. Böttger, L. Frey, and T. Mikolajick, "Ferroelectricity in simple binary ZrO2 and HfO2," Nano Lett. 12, 4318-4323 (2012).
- 30S. Mueller, J. Mueller, A. Singh, S. Riedel, J. Sundqvist, U. Schroeder, and T. Mikolajick, "Incipient ferroelectricity in Al-doped HfO2 thin films," Adv. Funct. Mater. 22, 2412-2417 (2012).
- 31 M. H. Park, Y. H. Lee, H. J. Kim, Y. J. Kim, T. Moon, K. D. Kim, J. Müller, A. Kersch, U. Schroeder, T. Mikolajick, and C. S. Hwang, "Ferroelectricity and antiferroelectricity of doped thin HfO2-based films," Adv. Mater. 27, 1811-1831
- ³²A. K. Saha, B. Grisafe, S. Datta, and S. K. Gupta, "Microscopic crystal phase inspired modeling of Zr concentration effects in Hf1-xZrxO2 thin films," in Symposium on VLSI Technology (IEEE, Kyoto, 2019), pp. T226-T227.
- 33E. Ko, H. Lee, Y. Goh, S. Jeon, and C. Shin, "Sub-60-mV/decade negative capacitance FinFET with sub-10-nm hafnium-based ferroelectric capacitor," IEEE J. Electron Devices Soc. 5, 306-309 (2017). .
- ³⁴F. A. McGuire, Y.-C. Lin, K. Price, G. B. Rayner, S. Khandelwal, S. Salahuddin, and A. D. Franklin, "Sustained sub-60 mV/decade switching via the negative capacitance effect in MoS2 transistors," Nano Lett. 17, 4801-4806 (2017).
- 35M. Si, C.-J. Su, C. Jiang, N. J. Conrad, H. Zhou, K. D. Maize, G. Qiu, C.-T. Wu, A. Shakouri, M. A. Alam, and P. D. Ye, "Steep-slope hysteresis-free negative capacitance MoS₂ transistors," Nat. Nanotechnol. 13, 24-28 (2018).
- 36H. Zhou, D. Kwon, A. B. Sachid, Y. Liao, K. Chatterjee, A. J. Tan, A. K. Yadav, C. Hu, and S. Salahuddin, "Negative capacitance, n-channel, Si FinFETs: Bi-directional sub-60 mV/dec, negative DIBL, negative differential resistance and improved short channel effect," in IEEE Symposium on VLSI Technology (IEEE, Honolulu, HI, 2018).
- ³⁷M. Si, C. Jiang, W. Chung, Y. Du, M. A. Alam, and P. D. Ye, "Steep-slope WSe₂ negative capacitance field-effect transistor," Nano Lett. 18, 3682-3687 (2018).
- 38D. Kwon, K. Chatterjee, A. J. Tan, A. K. Yadav, H. Zhou, A. B. Sachid, R. D. Reis, C. Hu, and S. Salahuddin, "Improved subthreshold swing and short

- channel effect in FDSOI n-channel negative capacitance field effect transistors," IEEE Electron Device Lett. 39, 300–303 (2018).
- 39 K. Ni, A. Saha, W. Chakraborty, H. Ye, B. Grisafe, J. Smith, G. B. Rayner, S. Gupta, and S. Datta, "Equivalent oxide thickness (EOT) scaling with hafnium zirconium oxide high-κ dielectric near morphotropic phase boundary," in *IEEE International Electron Devices Meeting (IEDM)* (IEEE, San Francisco, CA, 2019), 7.4.1–7.4.4.
- ⁴⁰A. K. Saha, K. Ni, S. Dutta, S. Datta, and S. Gupta, "Phase field modeling of domain dynamics and polarization accumulation in ferroelectric HZO," Appl. Phys. Lett. 114, 202903 (2019).
- ⁴¹K. Chatterjee, S. Kim, G. Karbasian, A. J. Tan, A. K. Yadav, A. I. Khan, C. Hu, and S. Salahuddin, "Self-aligned, gate last, FDSOI, ferroelectric gate memory device with 5.5-nm Hf_{0.8}Zr_{0.2}O_{.2} high endurance and breakdown recovery," IEEE Electron Device Lett. 38, 1379–1382 (2017).
- ⁴²S. Dünkel, M. Trentzsch, R. Richter, P. Moll, C. Fuchs, O. Gehring, M. Majer, S. Wittek, B. Müller, T. Melde, H. Mulaosmanovic, Stefan Slesazeck, S. Müller, J. Ocker, M. Noack, D-A Löhr, P. Polakowski, J. Müller, T. Mikolajick, J. Höntschel, B. Rice, J. Pellerin, and S. Beyer, "A FeFET based super-low-power ultra-fast embedded NVM technology for 22 nm FDSOI and beyond," in *IEEE International Electron Device Meeting* (IEEE, San Francisco, CA, 2017).
- ⁴³H. Mulaosmanovic, E. Chicca, M. Bertele, T. Mikolajickac, and S. Slesazecka, "Mimicking biological neurons with a nanoscale ferroelectric transistor," Nanoscale 10(46), 21755–21763 (2018).
- ⁴⁴H. Mulaosmanovic, J. Ocker, S. Müller, M. Noack, J. Müller, P. Polakowski, T. Mikolajick, and S. Slesazeck, "Novel ferroelectric FET based synapse for neuromorphic systems," in *Proceedings of IEEE VLSI Technology* (IEEE, Kyoto, 2017), pp. T176–T177.
- ⁴⁵M. Jerry, P. Chen, J. Zhang, P. Sharma, K. Ni, S. Yu, and S. Datta, "Ferroelectric FET analog synapse for acceleration of deep neural network training," *IEEE International Electron Device Meeting (IEDM)* (IEEE, San Francisco, CA, 2017), pp. 6.2.1–6.2.4.

- ⁴⁶K. Ni, B. Grisafe, W. Chakraborty, A. K. Saha, S. Dutta, M. Jerry, J. A. Smith, S. Gupta, and S. Datta, "In-memory computing primitive for sensor data fusion in 28 nm HKMG FeFET technology," in *IEDM Technology Digest* (IEEE, San Francisco, CA, 2018), pp. 16.1.1–16.1.4.
- ⁴⁷Y. Zhang, J. Sun, J. P. Perdew, and X. Wu, "Comparative first-principles studies of prototypical ferroelectric materials by LDA, GGA, and SCAN meta-GGA," Phys. Rev. B **96**, 035143 (2017).
- ⁴⁸W. Dinga, Y. Zhanga, L. Taob, Q. Yanga, and Y. Zhoua, "The atomic-scale domain wall structure and motion in HfO₂-based ferroelectrics: A first-principle study," Acta Mater. 196, 556–564 (2020).
- study," Acta Mater. 196, 556-564 (2020).

 49L. Landau and E. Lifshits, "On the theory of the dispersion of magnetic permeability in ferromagnetic bodies," Phys. Zeitsch. Sow. 8, 153-169 (1935).
- ⁵⁰C. Kittel, "Theory of the structure of ferromagnetic domains in films and small particles," Phys. Rev. 70, 965–971 (1946).
- 51 M. Hoffmann, F. P. G. Fengler, M. Herzig, T. Mittmann, B. Max, U. Schroeder, R. Negrea, P. Lucian, S. Slesazeck, and T. Mikolajick, "Unveiling the double-well energy landscape in a ferroelectric layer," Nature 565, 464–467 (2019).
- ⁵²J. Kittl, M. Houssa, V. V. Afanasiev, and J. Locquet, "Comment on 'Unveiling the double-well energy landscape in a ferroelectric layer'," Mesoscale Nanoscale Phys. (2020); arXiv:2003.00426.
- 53H.-J. Lee, M. Lee, K. Lee, J. Jo, H. Yang, Y. Kim, S. C. Chae, U. Waghmare, and J. H. Lee, "Scale-free ferroelectricity induced by flat phonon bands in HfO₂," Science 369, 1343 (2020).
- 54S. Gupta, M. Steiner, A. Aziz, V. Narayanan, S. Datta, and S. K. Gupta, "Device-circuit analysis of ferroelectric FETs for low-power logic," IEEE Trans. Electron Devices 64, 3092–3100 (2017).
- 55M. Jerry, J. A. Smith, K. Ni, A. Saha, S. Gupta, and S. Datta, "Insights on the DC characterization of ferroelectric field-effect-transistors," in 76th Device Research Conference (DRC) (IEEE, Santa Barbara, CA, 2018), pp. 1–2.